On light by light interactions in QED

Theoretical descriptions and experimental observations

Joel Thiescheffer

Supervised by Prof. Dr. Daniel Boer

Second examiner: Prof. Dr. Diederik Roest

rijksuniversiteit groningen

A thesis presented for the degree of
Bachelor of Science

Faculty of Science and Engineering
University of Groningen
The Netherlands
July 2017

On light by light interactions in QED

Theoretical descriptions and experimental observations

Abstract

In classical electrodynamics photons do not interact. However, in QED this becomes possible. The low energy effective field theory of Euler and Heisenberg is used to describe these interactions, which lead to non-linear corrections to the classical Maxwell equations in vacuum. The influence of effective QED light-by-light scattering on the polarization angle of light is discussed. Axions inducing a birefringence of the vacuum is mentioned. Recent experimental observations of the Very Large Telescope on the polarization angle and polarization degree of optical light from isolated neutron star RX J1856.5-3754 are compared to predictions of the Euler-Heisenberg Lagrangian in the weak field limit. A non-perturbative calculation could potentially yield better predictions. The measured values are too low to provide evidence for QED vacuum birefringence. Reduction of the experimental error in the future could lead to strong evidence for QED vacuum birefringence. In addition, possible observations on light-by-light scattering of the ATLAS collaboration at CERN are discussed. A non-zero virtuality and a diphoton invariant mass greater than 6 GeV exclude detection of real QED light-by-light scattering. ATLAS detects quasi-real QCD LbyL scattering. Better statistical information concerning the diphoton invariant mass spectrum around 10 GeV is necessary to conclude whether quasi-real QCD light-by-light scattering is detected at this point. At the moment, a diphoton detection from $\chi_{b,0}$ and $\chi_{b,2}$ diphoton decays cannot be excluded.

Contents

Chapter 1

Aim, structure and conventions

1.1 Aim and structure of this thesis

This work has two main aims. The first one is to give a theoretical description of interactions between photons within low energy effective field theory. The other one is to discuss claimed evidence of these interactions in recent experimental observations.

This work is roughly ordered as follows. First the reader is introduced to the concepts. Then it is explained how these concepts are theoretically formulated. The gained conceptual and theoretical knowledge are then applied to experimental observations.

1.2 Conventions

Most of the time units are used in which $\epsilon_0 = \mu_0 = \hbar = c = 1$, which are natural Heaviside-Lorentz units, although we switch a few times to SI units for physical purposes. The conversion to SI units is described in appendix A. Values of the fundamental constants in SI units are also included in Appendix A. As usual, Greek indices denote spacetime coordinates where the zeroth component is the temporal coordinate. Roman indices denote spatial coordinates.

Chapter 2

Non-linear QED effects

This chapter can be considered as an elaborate introduction to the topic of interactions between photons. It is centered around the question "how do photonic interactions become possible in quantum electrodynamics (QED)"? The answer to this question is found in the (quantum) nature of the vacuum. Meanwhile, important equations, expressions and concepts are defined. The structure is as follows. We start with a brief review of classical electrodynamics. We compare the classical vacuum with the Dirac vacuum and the QED vacuum. We do this in chronological order, following historical developments. Then we discuss examples of non-linear QED effects conceptually, with emphasis on the effects claimed to have been observed.

2.1 Interpretations of the vacuum

2.1.1 Classical theory of light

The majority of this review on classical electrodynamics is based on [1, 2]. The mathematical formulation of classical electromagnetism was due to James Clerk Maxwell. Maxwell published in 1861 and 1862 a set of linear partial differential field equations that relate the electric and magnetic fields to charges and currents. These equations describe light as a wave phenomenom. Before discussing the classical Maxwell equations describing light we define some quantities which will reappear throughout this thesis.

We define the following two antisymmetric, second-rank tensors

$$F^{\mu\nu} \equiv \partial^\mu A^\nu - \partial^\nu A^\mu \tag{2.1}$$

$$\tilde{F}^{\mu\nu} \equiv \frac{1}{2}\epsilon^{\mu\nu\alpha\beta}F_{\alpha\beta} \tag{2.2}$$

where $F^{\mu\nu}$ is the field strength tensor, $\tilde{F}^{\mu\nu}$ the dual tensor, $\epsilon^{\mu\nu\alpha\beta}$ the four dimensional Levi-Civita symbol and A^μ the four-vector electromagnetic potential. We made use of the Einstein summation convention i.e. a summation is implied over repeated indices. The field strength tensor is in itself not a fundamental field. It is constructed from derivatives of the gauge field A^μ. The fact that A^μ is a gauge field means we can add first order derivatives of any real-valued function to A^μ while still describing the same physics. The field tensors contain 6 independent components due to their

antisymmetry, which are the spatial components of the electric and magnetic field. Two of the Maxwell equations in vacuum can be derived from a Lagrangian. The Lagrangian is composed of the product of the electromagnetic field tensor

$$\mathcal{L}_{Maxwell} = -\frac{1}{4}F^{\mu\nu}F_{\mu\nu} \tag{2.3}$$

The Euler-Lagrange (EL) equation of motion for fields, which follows from Hamiltons principle of least action, takes the following form

$$\partial_\mu \frac{\partial \mathcal{L}}{\partial(\partial_\mu A_\nu)} - \frac{\partial \mathcal{L}}{\partial A_\nu} = 0 \tag{2.4}$$

Calculating the corresponding equation of motion yields

$$\partial_\mu F^{\mu\nu} = 0 \tag{2.5}$$

The other two Maxwell equations can be obtained through the Bianchi identity

$$\partial_\sigma F_{\mu\nu} + \partial_\mu F_{\nu\sigma} + \partial_\nu F_{\sigma\mu} = \partial_\mu \epsilon^{\mu\nu\alpha\beta} F_{\alpha\beta} = \partial_\mu \tilde{F}^{\mu\nu} = 0 \tag{2.6}$$

So in relativistic covariant notation the Maxwell equations in vacuum reduce to two equations

$$\begin{aligned} \partial_\mu F^{\mu\nu} &= 0 \\ \partial_\mu \tilde{F}^{\mu\nu} &= 0 \end{aligned} \tag{2.7}$$

These two equations encapsulate the more familiar Maxwell equations in differential form. These are

$$\begin{aligned} \nabla \cdot \vec{E} = 0 \quad &, \nabla \times \vec{B} = \frac{\partial \vec{E}}{\partial t} \\ \nabla \cdot \vec{B} = 0 \quad &, \nabla \times \vec{E} = -\frac{\partial \vec{B}}{\partial t} \end{aligned} \tag{2.8}$$

The first two equations are called Gauss's law and Ampère's law from left to right. The bottom right equation is called Faraday's law and the other one has no name. For completeness we state how A^μ is related to the electric and magnetic field

$$\vec{E} = -\nabla\phi - \frac{\partial \vec{A}}{\partial t} \quad , \vec{B} = \nabla \times \vec{A} \tag{2.9}$$

where ϕ, the scalar potential, denotes the temporal component of A^μ. Equations 2.8 describe the propagation of light in the vacuum. The linearity of the classical Maxwell equations has the important mathematical consequence that the superposition principle holds, i.e. any linear combination of solutions is also a solution to the equations. This implies that two photons cannot interact with each other. This is a somewhat strange statement since the concept of light as photons does not exist in classical electrodynamics. Instead, light is an electromagnetic wave. It is therefore better to say that when light is considered in a quantum mechanical framework, i.e. considering light as photons, then according to the classical Maxwell equations these particles cannot interact electromagnetically since they carry no electric charge.

The Maxwell equations lose their linearity in the fields, which means the superposition principle breaks down, when interactions between photons via virtual charged

fermion pairs are included. Interactions between photons are therefore called non-linear. We will get to this.

From equations 2.8 the classical wave equations can be derived for the electric and magnetic field. In SI units these read

$$\begin{gathered}\nabla^2 E = \epsilon_0\mu_0\frac{\partial^2 E}{\partial t^2} \quad ,\nabla^2 B = \epsilon_0\mu_0\frac{\partial^2 B}{\partial t^2} \\ c^2 \equiv \frac{1}{\epsilon_0\mu_0}\end{gathered} \tag{2.10}$$

where ϵ_0 and μ_0 are the electric permittivity and magnetic permeability of the vacuum and c the speed of light in vacuum. From the wave equations we observe that in the vacuum electromagnetic radiation always travels at the speed of light and that the electric permittivity and magnetic susceptibility are equal ϵ_0 and μ_0. As a consequence of non-linear QED contributions to the Maxwell equations, the resulting wave equations will also be different. Summarizing, the *classical* vacuum is empty concerning (charged) matter, which is the physical reason why photons do not interact. Mathematically, this is manifested in the linearity of the Maxwell equations.

2.1.2 Dirac's vacuum

This section and the next one uses historical facts from [1, 15]. Paul Dirac was the first physicist to give a quantum mechanical description of the vacuum. In 1928, Dirac published his relativistic theory of the electron. The equation he proposed was

$$(i\gamma^\mu\partial_\mu - m)\psi = 0 \tag{2.11}$$

This equation is known as the Dirac equation. Here i denotes the complex number and m the mass of the particle. γ^μ denote the Dirac gamma matrices. In this notation it is a four-vector of four 4×4 matrices. These objects are defined through the Clifford algebra. The mathematical structure of the gamma matrices is not important for this discussion. What is important is the interpretation of ψ. To begin with, Dirac published the equation in a different form

$$\begin{gathered}i\frac{\partial\psi}{\partial t} = -i\vec{\alpha}\cdot\nabla\psi + m\beta\psi = \hat{H}\psi \\ \vec{\alpha} \equiv -\gamma^0\vec{\gamma} \quad ,\beta = \gamma^0\end{gathered} \tag{2.12}$$

Note that Dirac wrote down his equation in the same form as the non-relativistic Schrödinger equation. He did this because he interpreted his equation as the relativistic version of the Schrödinger equation. This meant that ψ had to be the wavefunction for a single particle with spin. Then, when solving his equation, positive and negative energy solutions are obtained. But how can a free particle have a negative energy? Many physicists of Dirac's time thought the negative energy solutions were not physical. This seems rather obvious since if the negative energy solutions were physical a free electron could not be stable. An electron could always drop down to a more negative energy level. Thus, the energy spectrum is unbounded from below. To solve this unbounded *negative energy problem* Dirac proposed the

idea of what is called the 'hole' picture of the vacuum. According to Dirac, in the vacuum all the negative energy states are filled with electrons, so that only the levels with positive energies are accessible. These filled negative energy states are called the *Dirac sea*.

2.1.3 Consequences of the Dirac picture

This theory has remarkable consequences. A negative energy state could be excited to a positive energy state, leaving behind a hole. These holes could be associated with the anti-particles of electrons, which nowadays are called positrons. This process is called vacuum pair production and in those days it was also referred to as vacuum polarization[1]. The process can be thought of as creating matter by exciting the vacuum. It is analogous to the ionization of an atom. This was basically the birth of QED.

However, pair creation from the vacuum is only possible if the light has an enormous intensity. Consequently, this process of vacuum pair production, in which the pairs are real particles, requires extremely large electric field strengths. In 1931, it was Fritz Sauter who calculated this electric field strength at which electrons would tunnel out from the Dirac sea, producing pairs from the vacuum. It is this field strength that is defined as the *critical field* strength

$$E_{cr} \equiv \frac{m_e^2 c^3}{e\hbar} \approx 1.3 \times 10^{18} V/m \quad , B_{cr} = \frac{E_{cr}}{c} \approx 4.4 \times 10^9 T \tag{2.13}$$

where e is the elementary charge, $\hbar = \frac{h}{2\pi}$ the reduced Plank constant and m_e the electron mass. Today, for the electric field strength, it is called the *Schwinger limit*. At field strenghts above the Schwinger critical field strength it is expected that vacuum pair production effects become important.

Very soon after this, Werner Heisenberg started investigating this new theory of Dirac. In 1927, Heisenberg had introduced his uncertainty principle. For energy and time it takes this form

$$\Delta E \Delta t > \frac{\hbar}{2} \tag{2.14}$$

He realized that his uncertainty principle shows that in order to produce pairs from the vacuum, it is sufficient to use electromagnetic field strenghts below the Schwinger limit, due to the virtual possibility of creating matter. This refers to the production of *virtual* particles. Due to their limited existence in time governed by the uncertainty in energy, these particles are called virtual. He developed in two papers this formalism of what he called *quantum fluctuations* from the Dirac sea. Two Phd-students of Heisenberg, Hans Euler and Bernhard Kockel computed the leading corrections to the Maxwell theory. These leading corrections corresponded to interactions between photons via virtual charged pairs, leading to new quantum phenomena. This will be the main topic in this thesis. They suggested in that paper that the vacuum could be interpreted as a medium and that it thus can be

[1]Nowadays vacuum polarization is a concept within quantum electrodynamics. It is still associated with pair-production, but not of real pairs but virtual pairs. We will discuss this concept in section 2.2.

polarized. In 1936 Heisenberg and Euler obtained a closed-form integral expression of the non-linear corrections to the Maxwell Lagrangian [20]. This correction is today known as the Euler-Heisenberg (EH) Lagrangian, which will be the topic of the next chapter. Nowadays, we would call this method of Heisenberg and Euler a low energy effective field theory, since they restricted their calculations to a particular energy scale. With this result, Heisenberg and Euler were able to predict the instability of the QED vacuum in the presence of a background field. They made it clear that background electric fields give rise to different physical effects compared to a magnetic field background. Critical electric fields could produce real pairs from the vacuum and magnetic fields could lead to dispersive effects such as birefringence and dichroism. Note that for these dispersive QED effects *critical* magnetic fields are not necesarry. For a detailed discussion on the effects caused by critical magnetic fields the reader is referred to [16].

Today we know that ψ cannot be a single-particle wavefunction since particle number is not conserved in nature and the notion of a single particle does not make sense, especially not at length scales shorter than the Compton wavelength for electrons

$$\lambda_c \equiv \frac{h}{m_e c} \approx 2.4 \times 10^{-12} m \tag{2.15}$$

where the probability of electron-positron pair production from the vacuum is high. Consequently, also the interpretation regarding the nature of the vacuum cannot be true. Although the Dirac equation was interpreted in the wrong way in those days, it led to the right predictions. A few manifestations of light-by-light interactions have been indirectly observed as QED contributions [5, 22, 33]. It is therefore safe to say that Heisenberg and Euler where far ahead of their time. 80 years later, new evidence is claimed for some of the phenomena predicted by Euler and Heisenberg in the 30s, which is the topic of chapter 4.

But since this interpretation of ψ is wrong, what does ψ then represent? And what are the consequences for the interpretation of the vacuum? This brings us to quantum field theory.

2.1.4 The vacuum as a quantum state

One of the main motivations to construct quantum field theory (QFT) was to reconcile the principles of special relativity with those of quantum mechanics. The merge of the mass-energy equivalence principle of Einstein and the uncertainty principle of Heisenberg is that particle number is not conserved, as we mentioned above. To get to the interpretation of ψ in QFT we first need to define what a (real) particle actually is. In QFT real particles are no longer fundamental, they are excitations of the underlying corresponding quantum fields. For example, the quantization of a real scalar field gives rise to spin-0 particles, which are bosons. Quantization of spinor/Dirac fields gives rise to spin-1/2 particles, which are fermions. Thus, ψ is a classical field that has to be quantized. But what about the vacuum? In QFT the vacuum is a quantum state denoted by $|0\rangle$ in the case for a free field[2]. When the quantum field is in its vacuum state it contains no real particles. The field is in its

[2]This means we do not consider interactions between particles.

lowest energy configuration. We could also define the vacuum state as the ground state of the field.

It should be said that this is quite a remarkable state. It contains an infinite amount of positive or negative energy depending on the field which is quantized. This is a direct consequence of the zero-point energy of a quantum harmonic oscillator. In QFT every spacetime point is considered a quantum harmonic oscillator. The total energy is an infinite sum of zero-point energies yielding an infinite energy for the vacuum state. This *vacuum energy* is neglected in QFT by subtraction from the Hamiltonian since it is impossible to measure the energy of the vacuum state directly. However, as a consequence of the Heisenberg uncertainty relation for energy and time, fluctuations in the vacuum energy, by which we mean virtual particles, could in principle be detected. The Casimir effect is usually given as evidence for the presence of vacuum energy fluctuations. However, this is a matter of interpretation[3]. In this thesis we discuss photon-photon interactions which couple via virtual charged pairs and therefore a detection of such a process would be direct evidence for the presence of vacuum fluctuations. This picture of the vacuum where fluctuations in the vacuum energy take place is called the quantum vacuum. In the case of considering leptonic electrically charged fluctuations (electron-positron pairs) the quantum vacuum is called the *QED vacuum*. The appearance of these virtual particles seems to be a violation of conservation of energy but according to the Heisenberg uncertainty relation for energy and time, energy conservation is allowed to be violated constraint by the uncertainty in time. Then, according to the equivalence between mass and energy this means that particles can be produced. This production of virtual pairs is sometimes explained as if energy is "borrowed" from the vacuum energy. The probability of producing virtual electron-positron pairs starts to become high at length scales of the order of the electron Compton wavelength, the typical scale of relativistic quantum mechanics.

The difference between the QED vacuum and the Dirac vacuum is that in the QED vacuum the infinite amount of negative charge has been removed and that positrons are real particles, instead of holes. Actually, the physical picture of vacuum fluctuations in the context of the Dirac vacuum seems not extremely different from the QED picture. In fact, considering the vacuum from a QED perspective, when the vacuum is subject to a constant[4] external field, the situation is the same in both physical pictures. The true physical nature of the vacuum remains an open question in modern physics. Now that we have discussed the appearance of virtual particles we can discuss *vacuum polarization* in a QFT framework.

[3]The Casimir effect is often used in textbooks as the example of evidence for the existence of vacuum fluctuations. However, this is a matter of interpretation since there is another explanation possible which does not make use of vacuum fluctations.

[4]Actually, slowly varying fields are allowed. Later on, we will specify what is meant by "slowly".

2.2 Vacuum polarization and the mass-shell

In the previous section vacuum polarization referred to pair production from the vacuum. It still does, but now in a field theoretic framework. Vacuum polarization refers to the pair production of virtual pairs from photons. Vacuum polarization is one aspect of the self-energy of the photon. It refers to the loop arising in the photon propagator (see figure 2.1). The fermion anti-fermion loop can be formed by any

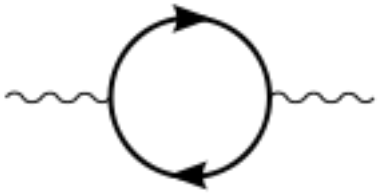

Figure 2.1: Diagram of vacuum polarization ($\gamma \to \gamma$). A photon becomes a fermion anti-fermion pair which subsequently annihilates to a photon.

charged fermion pair. After the constraint time due to the uncertainty principle, the virtual particles annihilate each other to form again a photon. All non-linear QED phenomena originate from vacuum polarization. Two photons can couple via this charged virtual particle loop. This is the reason why one also speaks of *vacuum polarization effects*, when discussing interactions between photons. The term *polarization* might give the idea that the vacuum is a polarizable medium. Indeed, due to the presence of virtual particles and an external magnetic field the QED vacuum possesses properties of ordinary media, like birefringence and dichroism. It is important to emphasize that the QED vacuum is different from ordinary classical dielectric media. Its "medium" properties arise through non-linear QED effects. We will see that the resulting modified Maxwell equations remind of the Maxwell equations in matter.

Vacuum polarization gives rise to charge renormalization. Since particle number is not conserved a real particle is always surrounded by virtual (electrically) charged pairs. These virtual particles are referred to as "screening" particles. The electric charge of a particle increases as one approaches the particle. The electric charge becomes distance (or energy) dependent. The electromagnetic coupling strength between electrically charged particles and the electromagnetic field is characterized by the fine-structure "constant" α. However, since the electric charge of a particle depends on distance, this also implies a distance dependent fine-structure constant $\alpha(r)$. At distances large compared to the electron Compton wavelength (or energies far below the electron mass) α has the familiar value of approximately $\alpha \equiv \frac{e^2}{4\pi\epsilon_0\hbar c} \approx \frac{1}{137}$ and it can be considered constant. However, at smaller Compton wavelengths (higher energies), the value of α increases. We will be interested in energies far below the electron mass of 0.5 MeV.

A note on virtual particles

Until now, we have spoken a bit losely about the nature of a virtual particle, though we mentioned its lifetime is determined by an energy uncertainty. Let's look a little closer at what a virtual particle actually is. These virtual particles can be regarded as quantum vacuum fluctuations as mentioned before. At any spacetime point there is a non-vanishing probability amplitude for a photon to fluctuate into a pair. In this interpretation energy and momentum are "conserved" in some sense as we have seen but Einstein's energy-momentum relation is not obeyed, that is

$$E^2 = p^2 + m^2 \tag{2.16}$$

where p denotes the spatial momentum and m the invariant mass. These particles are called *off-shell* while particles that do obey this relation are called *on-shell*. Obeying this equation means we call a particle on-shell when its invariant mass is greater than zero. Photons are of course on-shell when their invariant mass equals zero. When a particle is on-shell it is a real particle. When it is off-shell it is called a virtual particle. Let's explain this terminology. When plotting equation 2.16 you get either a parabolic surface for massive particles or a cone for massless particles. This is the mass-shell. Real particles have their momentum vectors lying on the surface of the shell. When considering a collision between two particles, conservation of momentum requires that the vectorial sum of the initial situation equals the vectorial sum of the final situation. Consequently, the sum of the two vectors does not lie along the shell's surface, but it lies inside the surface. The presence of virtual particles solves this problem. They can be used to keep track of the total momentum in the system. Off-shell particles usually correspond to the internal lines in Feynman diagrams but this is not necessarily true in interactions between photons as we will see. External photon lines can correspond to virtual photons. When we come to light-by-light interactions it is actually crucial whether the photons participating in the interaction are on-shell or off-shell. Actually, it will become clear that it is experimentally impossible to create perfectly on-shell photons. Experimentally, the best thing (yet) to do is to minimize the virtuality of the photons. Therefore, we make a distinction between virtual photons and *quasi-real* photons. Whether a photon is called quasi-real or virtual depends on whether the virtuality is small compared to the energy in the center of mass system. This is discussed in more detail in section 4.2.2.

2.3 Examples of QED effects

Now that we have discussed the nature of the quantum vacuum and concepts like vacuum polarization and virtual particles, we have set the stage for quantum effects. Here we discuss examples of such non-linear effects conceptually. We separated the light-by-light QED effects from the Schwinger effect because the Schwinger effect is a non-perturbative QED effect while the other discussed effects are perturbative. We will elaborate on vacuum birefringence in a separate section since this requires some background knowledge from classical optics.

2.3.1 Light-by-Light interactions

Light-by-light (LbyL) interactions appear in various forms. In general, it refers to the reaction $\gamma\gamma \to \gamma\gamma$. Photons can scatter off each other or they can scatter in the electric field of a nucleus (Delbrück scattering). A photon can also interact with a magnetic field (vacuum birefringence) or a single photon can split into two photons in a magnetic field (photon-splitting). Photons can interact via quark-antiquark ($q\bar{q}$) loops, form an intermediate particle and subsequently decay into two photons (hadronic resonances). These are all examples of LbyL interactions. There are several experiments to study these photonic interactions. What is crucial is if the photons participating in the interaction are on-shell or off-shell and if the photons interact with a magnetic field or an electric field. This in essence determines which LbyL interaction takes place. We are going to discuss all the above mentioned LbyL interactions, though not all in full detail.

General remarks on one-loop diagrams and terminology

LbyL interactions can be written down in a first order approximation as one-loop Feynman diagrams (see figure 2.2 and figure 2.3) as a consequence of vacuum polarization. A photon interacts with another photon via the vacuum polarization of the other. One sees that the presence of virtual particles can be probed by coupling them to additional photons.

We want to make some important remarks on these one-loop Feynman diagrams, i.e. on the external photon lines and the internal lines constituting the loop. This will prevent confusion since very different physical effects are represented by very similar diagrams. We take for this example the box-diagram in figure 2.2, which is probably the best known to the reader. This diagram depicts photon-photon scattering via virtual charged (whether electrically or color and electrically charged) particles. Concerning the photon lines there are two remarks. The first one is that the photons can be either virtual, quasi real (both off-shell) or real (on-shell). Thus, it is for instance possible to scatter virtual photons with real photons. The second one is that it is important to see whether a photon originates from an external electric field or a magnetic field. For example, when one of the incoming photons originates from a magnetic field, it is really a different physical LbyL interaction than photon-photon scattering. We will discuss this in more detail in the next section. Which virtual charged particles form the loop depends on the energies of the photons involved.

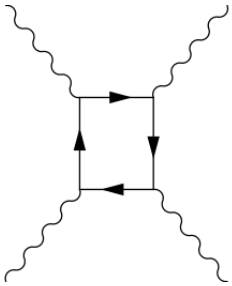

Figure 2.2: Photon-photon scattering.

In this thesis we are interested in interactions between low energy photons with respect to (w.r.t.) the electron mass of 0.5 MeV. At low initial photon energies a LbyL interaction is mediated by electron-positron (e^+e^-) pairs. When the loop consists of e^+e^- pairs in a photon-photon scattering process we define this process as *QED LbyL scattering*. This is the process predicted by Euler and Heisenberg. For photon energies far below the electron mass, the photon-photon scattering process can be described by the Euler-Heisenberg Lagrangian, which is a low energy effective field theory. We discuss this in chapter 3, in section 3.1. At photon Center of Mass (CoM) energies approaching the electron mass and higher this process has to be treated within a complete QED framework. Meanwhile, at increasing photon energies, light $q\bar{q}$ loops such as $u\bar{u}$ and $d\bar{d}$ loops start to dominate over e^+e^- loops. When the loop consists of $q\bar{q}$ pairs we refer to this LbyL scattering process as *QCD LbyL scattering*, where QCD stands for Quantum ChromoDynamics. In the literature, for example in [11, 7], the definition of QED LbyL scattering is not restricted to e^+e^- loops but it refers to any charged fermion or boson loop (W^+W^- loops). We make this distiction between QED and QCD LbyL scattering since quarks carry besides electric charge also color charge and therefore in addition to the electromagnetic interaction they also interact via the strong interaction. The strong interaction is described by QCD, hence the name QCD LbyL scattering. We are only interested in low photon energy QED effects. Other charged lepton loops, i.e. $\mu^+\mu^-$ and $\tau^+\tau^-$, are suppressed in the Euler-Heisenberg Lagrangian since this Lagrangian can be expanded in powers of $\frac{E_\gamma}{m_e}$. Since $\frac{E_\gamma}{m_e} \gg \frac{E_\gamma}{m_\mu} \gg \frac{E_\gamma}{m_\tau}$ these loops are suppressed. Here E_γ denotes the center of mass energy the photons. For the same reason all $q\bar{q}$ loops are suppressed. Thus, we restrict ourselves to low photon energies and therefore only to e^+e^- loops.

Thus, the prefix QED or QCD refers to the charged particle pairs constituting the loop which couples the four photons. Although we mentioned to be only interested in e^+e^- loops, we included this discussion on $q\bar{q}$ loops in anticipation of the ATLAS experiment discussed in chapter 4, which involves photon CoM energies that exceed the electron mass by several orders of magnitude. At these energies $q\bar{q}$ loops dominate over e^+e^- loops.

Scattering, splitting and vacuum birefringence

Figure 2.3 shows the one-loop diagrams of various LbyL interaction processes. The left diagram illustrates Delbrück scattering. Delbrück scattering is the deflection of on-shell photons in the electric field of nuclei[5]. Delbrück scattering can be considered a first approximation to photon-photon scattering (figure 2.2, right diagram in figure 2.3), as one ingoing and one outgoing photon are replaced by photons from the electric field of a nucleus [22]. This one-loop diagram is known to contribute as a QED correction [22]. The same Feynman box diagram also depicts vacuum birefringence. But in the case of vacuum birefringence the crosses denote an external magnetic field instead of an electric field of a nucleus. This illustrates the importance of keeping track of the physics behind the diagram. Why this effect is called "vacuum birefringence" is the topic of the next section.

An effect closely related to vacuum birefringence, in that an on-shell photon interacts with an external magnetic field, is photon splitting. In an external magnetic field a photon can split into two photons ($\gamma \to \gamma\gamma$). It is depicted in the diagram in the middle of the figure below. This box diagram has also been observed as a QED contribution in [22].

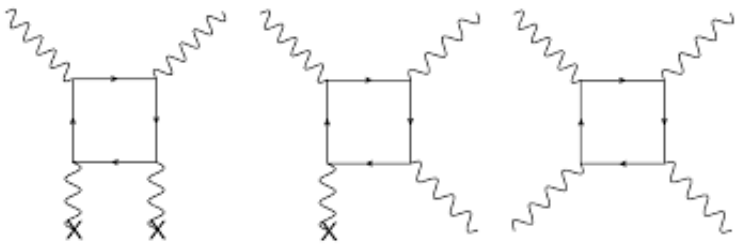

Figure 2.3: The left diagram illustrates Delbrück scattering or vacuum birefringence depending on whether the crosses denote an electric field of a nucleus or an external magnetic field respectively. The right diagram illustrates elastic photon-photon scattering. The middle one is a diagram of photon splitting (the cross here denotes a magnetic field). These are one-loop diagrams. The diagrams correspond to the leading order correction in the perturbative expansion of the Euler-Heisenberg effective Lagrangian. This image is taken from [11].

In the case of on-shell elastic QED photon-photon scattering there is no notion of virtual photons. This process is depicted in the right diagram of figure 2.3. All these photons are real/on-shell. It is important to emphasize under which physical conditions this process takes place. This is a regime of low photon energy w.r.t. electron mass. In particle accelerators, such as the Large Hadron Collider (LHC), the high energy (and high intensity) QED regime can be probed. However, to test real QED LbyL scattering this is not desired. Another problem that arises in particle collision experiments (and any other experimental setup which studies real LbyL scattering) is that it is not known how to create perfectly on-shell photons. Colliding

[5]The photons originating from the electric field of nuclei are highly off-shell, unless it is an ion.

laser beam experiments can probe the optical energy regime such that the photons can be considered more on-shell. However, here the cross section forms a problem. In chapter 3 we will see that real QED LbyL scattering has an extremely small cross-section. Real QED LbyL scattering is still an unobserved process, just as real QCD LbyL scattering. QED LbyL scattering has been measured indirectly as one of the contributions to the anomalous magnetic moment[6] of the muon and the electron [5]. But this contribution was not fully real QED LbyL scattering. This is indirect evidence for the existence of the e^+e^- loop. In [27] experimental suggestions are given to create almost real QED LbyL scattering events using lasers, each with its benefits and disadvantages. In the previous section we mentioned that photons can also be considered quasi-real. In this case, we do not necessarily have to perform extremely low energy experiments, since whether a photon is considered quasi-real does not imply its energy is low. Consequently, the low value of the cross section is no longer a problem.

The ATLAS collaboration at CERN claims to have observed evidence for LbyL scattering directly [11]. Note that they do not claim to have seen *real* LbyL scattering. It is thus also possible to scatter two off-shell photons with each other, which can be virtual or quasi-real. It is illustrated by the same box-diagram. Therefore, we make this distinction between off-shell (virtual or quasi-real) and on-shell (real) LbyL scattering. In this thesis we are interested in whether real QED LbyL scattering is detected. This is of more interest than real QCD LbyL scattering for two reasons. Quark loops have already been observed, though also indirectly, in a wide variety of processes, for example in π^0 decay (see figure 2.4). But what is probably more important is that the detection of real QED LbyL scattering would prove a fundamental difference between QED and Maxwells electromagnetism. It is this process that has to be compared to the classical theory since classical electromagnetism predicts that real LbyL scattering is impossible. In addition, it would be evidence for the existence of the e^+e^- loop, i.e. evidence for fluctuations in the vacuum energy, though this could also be proven in off-shell QED LbyL scattering. Whether real QED LbyL scattering is detected by ATLAS will be discussed in chapter 4.

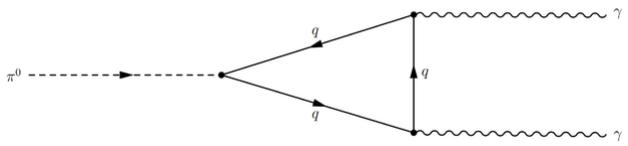

Figure 2.4: Neutral pion decay via a quark loop.

[6]The QED deviation from the value of 2 predicted by Dirac.

Hadronic resonances and axions

In anticipation of discussions in chapter 4 we include here a short discussion on hadronic resonances and axion-photon coupling. When the initial photons have sufficient energies they can also interact with each other via the production of an intermediate particle, which subsequently decays into two real photons. This intermediate state is referred to as a *hadronic resonance*. It is a bounded state with a finite lifetime. Two off-shell photons interact via a $q\bar{q}$ loop and form a hadronic resonance. It is also referred to as a *photon-fusion* process. It is not necessarily the case that a hadronic resonance decays into two photons. The *Landau-Yang theorem* states that a spin-1 resonance state cannot decay into two on-shell photons. However, in chapter 4 we will be interested in hadronic resonances that are able to decay into two photons. One could ask what kind of particle a hadronic resonance is. Which particle is produced depends on the energies of the photons. These particles include mesons, which are hadrons composed of $q\bar{q}$ pairs. Only mesons composed of a quark and its antiquark can be produced. A familiar example is the already mentioned neutral pion (π^0), composed of a linear combination of an up anti-up ($u\bar{u}$) pair and a down-antidown ($d\bar{d}$) pair. The u, d and strange (s) quarks are much lighter than the charm (c), bottom (b) and top (t) quarks. Therefore, the π^0 exists in a quantum mechanical superposition of $u\bar{u}$ and $d\bar{d}$ pairs. Hadronic resonances can also be com-

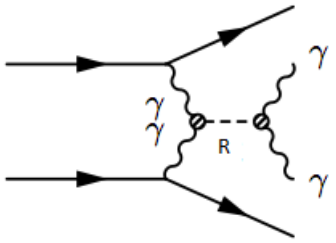

Figure 2.5: Creation of a hadronic resonance, denoted by 'R', via a $q\bar{q}$ loop in the collision of two particles. Two particles emit off-shell photons which fuse to form an intermediate quarkonium state which then decays into two on-shell photons if it has a spin different from 1.

posed of pairs of the heavier quarks, like $c\bar{c}$ and $b\bar{b}$. These particles are composed of one $q\bar{q}$ flavor. The $t\bar{t}$ (toponium) state is not observable since it decays too fast into other mesons. We also refer to these heavier hadronic resonances as *quarkonia*. Quarkonia come about in different (excited) states. This means that there exists a whole collection of, say $c\bar{c}$ resonances with different term symbols, referring to different $c\bar{c}$ bound states. This is similar to the term symbols associated to atomic energy levels. These term symbols depend on the quantum numbers n, L, S and J, with J=L+S. These denote the principal, orbital angular momentum, spin angular momentum and total angular momentum quantum number respectively. For instance, the ground state of the J/Ψ-meson, denoted by J/Ψ(1S), is a particular state of charmonium ($c\bar{c}$) with S=J=1 and n=L=0. Since J/Ψ has S=1, diphoton decay is forbidden according to the Landau-Yang theorem. Several experiments in the past have observed hadronic resonances in e^+e^- collision experiments, for instance [4, 33].

To conclude this section on LbyL interactions we end with another unobserved process involving a new hypothetical particle, which is called the axion. An axion is either a pseudoscalar or scalar[7] spin-zero boson, proposed to solve the so called *strong CP-problem*[8] in the standard model [12]. In the laboratory there is a particular elegant experimental setup, which makes use of a photon-axion oscillation process in the presence of a strong magnetic field. These are the so called *light shining through a wall* (LSW) experiments [30]. The interested reader is referred to [30]

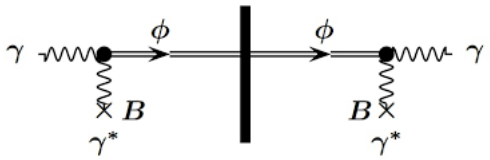

Figure 2.6: Light shining through a wall experiment. A photon interacts with a magnetic field to form an axion (ϕ), which is a spin-zero boson. The axion moves through a wall and then decays again into two photons in a magnetic field.

for a detailed discussion on axion searches. The coupling strength between axions and photons is characterized by an axion-photon coupling constant $|G|$, which is currently less than 10^{-10} GeV^{-1} based on astrophysical considerations [19]. Until now, axions remain unobserved. We will meet axions later on again in the context of vacuum birefringence, which we are going to discuss now in more detail.

2.3.2 Vacuum birefringence

We already mentioned that photons interacting with external magnetic fields and photon-axion coupling induce a new quantum phenomenon called *vacuum birefringence*. As the name suggests, it refers to the vacuum having two indices of refraction corresponding to two orthogonal polarization modes, just as classical optics predicts that assymmetric dielectric media can be birefringent. We start this discussion on vacuum birefringence with the relevant classical concepts like ordinary birefringence and polarization. Information about classical optics can be found in any optics textbook, for example in [3].

Stokes parameters

In anticipation of the analysis in section 3.5.1 we discuss the Stokes parameters. Light can be in different states of polarizations (SOP). There are three distinct polarizations possible; linear, circular and elliptical polarization. Polarization refers by convention to the direction of the electric field vector. In the case of linear polarization the electric field vector is restricted to lie in a plane called the plane of vibration or polarization plane. The orientation of the electric field vector can thus be considered constant and its magnitude is allowed to vary with time. Consider two linearly polarized harmonic waves with their electric fields perpendicular to each

[7] If the axion is a scalar particle, it would not solve the strong CP-problem.
[8] The question why the QCD Lagrangian conserves CP-symmetry.

other. When superimposing these harmonic waves, the SOP of the resulting wave is then determined by the phase difference between the initial waves. Linear and circular polarized light are special cases of elliptical polarized light. This means that in general the electric field vector will not lie in a plane and change its magnitude, tracing out an ellipse during an oscillation, in a fixed space perpendicular to the direction of propagation. A polarization state can then be described by the geometrical parameters of an ellipse and the direction of oscillation which is called the *handedness*. Describing a SOP using the geometry of the polarization ellipse

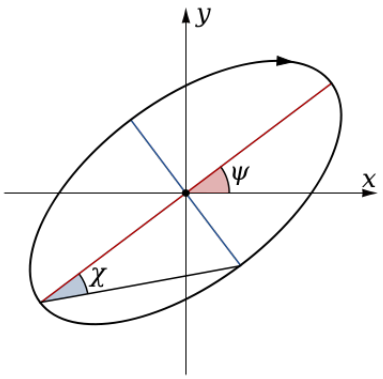

Figure 2.7: The polarization ellipse. ψ denotes the polarization position angle/orientation angle and χ the ellipticity angle. The Cartesian coordinates x and y denote the orthogonal linear polarization modes in these directions.

leads us to the definition of the Stokes parameters. Formally, the Stokes parameters are defined as intensities, i.e. they are time averages of electric fields. Consider a wave propagating in the $\hat{z}$-direction. This means that the electric and magnetic field oscillate in the $x - y$ plane.

$$\vec{E} = (E_{0x}e^{i\phi_x}\hat{x} + E_{0y}e^{i\phi_y}\hat{y})e^{-i\omega t} \tag{2.17}$$

Here denote E_{0x} and E_{0y} the amplitude in the x and y direction and ϕ_x and ϕ_y are the initial phases. The Stokes parameters are then defined as follows

$$\begin{aligned} I &\equiv \langle E_x^2 \rangle + \langle E_y^2 \rangle \\ Q &\equiv \langle E_x^2 \rangle - \langle E_y^2 \rangle \\ U &\equiv \langle 2E_x E_y \cos(\phi_x - \phi_y) \rangle \\ V &\equiv \langle 2E_x E_y \sin(\phi_x - \phi_y) \rangle \end{aligned}$$

where U and Q characterize the linear polarization, I the total intensity of the radiation and V measures the elliptical polarization. Using the angles defined in figure 2.7 the Stokes parameters are defined as follows:

$$\begin{aligned} I &= I_0 \\ Q &= I_0 \cos 2\chi \cos 2\psi \\ U &= I_0 \cos 2\chi \sin 2\psi \\ V &= I_0 \sin 2\chi \end{aligned} \tag{2.18}$$

The parameters I and V are independent of the coordinate system used since they are not functions of ψ while Q and U are dependent on the orientation of the x and y axes. Thus, the Stokes parameters describe a SOP in terms of intensities and two angles of the polarization ellipse. The Stokes parameters can be considered as forming a Cartesian coordinate system and I_0, 2ψ and 2χ a spherical coordinate system (where 2ψ is the polar angle and 2χ the azimuthal angle respectively). This means a SOP can be visualized as a vector in Poincaré space, i.e. a vector inside a sphere which is called the *Poincaré sphere*. The factors of two before the angles

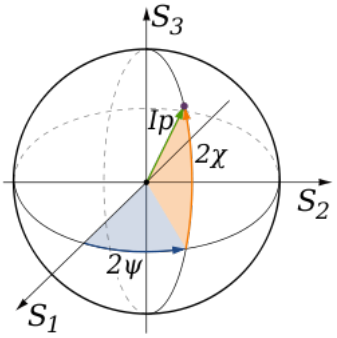

Figure 2.8: The Poincaré sphere. S_1, S_2 and S_3 denote Q, U and V respectively. I_p is the degree of polarization, which is called I_0 in our notation. It is the length of the Poincaré vector.

indicate that a π rotation gives the same ellipse and that we can swap the semi-major and minor axes and rotate by $\frac{\pi}{2}$ to get the same ellipse. Transforming back to a basis of ψ and χ we get the polarization angle and ellipticity angle as functions of the Stokes parameters:

$$\begin{aligned} I &= I_0 \\ \psi &= \frac{1}{2}\tan^{-1}\left(\frac{U}{Q}\right) \\ \chi &= \frac{1}{2}\tan^{-1}\left(\frac{V^2}{\sqrt{Q^2+U^2}}\right) \end{aligned} \tag{2.19}$$

ψ indicates the orientation of the polarization plane. In the experiment we are going to discuss on vacuum birefringence in chapter 4, a rotation of the polarization plane ($\Delta\psi$) is one of the measured quantities. The other is the linear polarization degree defined by

$$P_L \equiv \sqrt{Q^2+U^2} \tag{2.20}$$

It is the magnitude of the linear polarization vector, which is an invariant quantity under the orientation of the coordinate system (it is *psi* independent). One can normalize the Stokes parameters by dividing each one by the first parameter. The normalized linear polarization vector then becomes

$$P_L = \sqrt{\left\{\frac{Q}{I_0}\right\}^2 + \left\{\frac{U}{I_0}\right\}^2} \equiv \sqrt{P_Q^2 + P_U^2} \tag{2.21}$$

Birefringence

We start with an explanation of *birefringence*. When light travels through an anisotropic medium its refraction not only depends on how the light is incident on the medium but also on how it is polarized. The part of the wave with its electric field vector perpendicular to the optical axis[9], behaves as if the medium is isotropic. Light expands in all directions with phase velocity $v_\perp$. This is called the *o-wave*. In contrast, the part of the wave with polarization orthogonal to the polarization of the *o*-wave has a part in the direction of the optical axis and travels with phase velocity $v_\parallel$ where $v_\perp \neq v_\parallel$. This is called the *e-wave*[10]. So we see that a birefringent material contains two indices of refraction, due to the polarization dependent phase velocities. The amount of birefringence is characterized by the differences of the two indices of refraction: $\Delta n = n_e - n_o$.

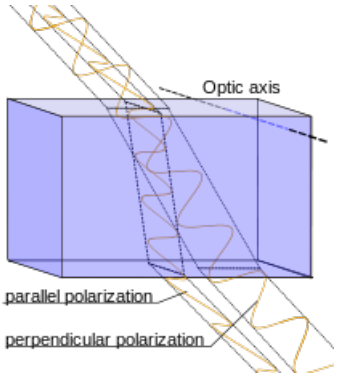

Figure 2.9: An image of birefringence.

Vacuum birefringence

We have seen that photons can interact with an external magnetic field via virtual charged particles. This effect gives the QED vacuum properties of dielectric media. Indeed, considering this photon-magnetic field interaction via virtual e^+e^- loops, the QED vacuum contains two different indices of refraction corresponding to two mutual orthogonal photon polarization modes. This is why one speaks of (QED) *vacuum birefringence*, though physically it of course differs from ordinary birefringence. While ordinary birefringence is a consequence of an anisotropic arrangement of atoms, vacuum birefringence is a consequence of vacuum polarization effects. More precisely, it is a consequence of the interaction between a photon and a magnetic field according to the corresponding one-loop diagram. The polarization state of a photon can be described as a superposition of mutual orthogonal linear polarized states. The polarization mode polarized parallel to the external magnetic field travels with a different phase velocity through the QED vacuum compared to the polarization mode polarized orthogonal to the magnetic field. Thus, in the case of vacuum birefringence the optical axis is the magnetic field axis. Note that this shows that light slows down in the presence of a magnetic field, i.e. $v_\perp < c, v_\parallel < c$

[9]The optical axis or principal axis is the direction about which the atoms are arranged symmetrically.

[10]*o* stands for *ordinary* and *e* stands for *extraordinary*.

and $v_\perp \neq v_\parallel$.

We already mentioned that when looking for experimental evidence for QED vacuum birefringence one could look for variations in the polarization state of light, for instance rotations of the polarization plane, i.e. $\Delta\psi \neq 0$, when only taking into account LbyL interactions. This is what the PVLAS collaboration since 2000 tries to detect using lasers. They continuously observed in experiments from 2000-2005 induced ellipticities and rotations by 5T magnetic fields on initially linearly polarized light travelling a distance of 1m through vacuum. However, the observed variations in the polarization state where orders of magnitude larger than predicted by the Euler-Heisenberg Lagrangian [34]. Recently, new evidence is claimed for QED vacuum birefringence in [29], which we are going to discuss in chapter 4.

2.3.3 Schwinger pair-production

We have seen that fluctuations in the vacuum energy lead to the production of virtual pairs. The Schwinger effect is an effect dealing with pair-production from the vacuum of electrons and positrons through an external critical electric field. An external critical electric field can accelerate the virtual pairs of electrons and positrons and finally split them from each other. These virtual pairs of electrons and positrons then become real pairs if they gain the energy of twice the electron mass from the critical electric field over a Compton wavelength. You can think of this process as an energy "payback" by the external electric field for the " borrowed" vacuum energy due to the virtual e^+e^- pair. The Schwinger effect has a non-perturbative dependence on the electric field which means it cannot be described by pertubative methods like Feynman diagrams. The non-perturbative dependence on the field causes difficulties for the experimentalist because of the exponential suppressing of the probability of the Schwinger effect. The leading exponential part of the probability of producing real pairs from the vacuum is proportional to [14]

$$P \propto \exp\left[-\frac{\pi m_e^2 c^3}{eE_{cr}\hbar}\right] \tag{2.22}$$

Squaring the critical field strength gives an estimate for the critical intensity: $I_c \propto E_c^2$. This yields an intensity of about $10^{33}W/m^2$. Current lasers are not able to reach this enormous intensity. The Extreme Light Infrastructure (ELI) project has lasers reaching intensities of about $10^{29}W/m^2$ [14]. This is still four orders of magnitude less than the critical intensity. It seems that for direct observation of Schwinger pair production we have to wait until the laser can reach the critical intensity. We are not going to discuss the Schwinger effect in more detail. For a more extended (theoretical) discussion on the Schwinger effect the reader is referr ed to [14] and references there in.

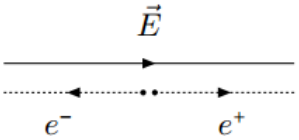

Figure 2.10: The Schwinger effect. An external electric field accelerates virtual e^+e^- pairs apart such that they become real pairs.

Chapter 3

Formalism

This chapter discusses the Euler-Heisenberg Lagrangian and its consequences. This is a low energy effective field theory. We start with a motivation why an effective field theory is used and with some general remarks on non-linear theories of electrodynamics (NLEDs). Then we discuss the Euler-Heisenberg Lagrangian and express it as a power series in the field tensor and its dual tensor. We compute the modified Maxwell equations to first order and the resulting modified wave equations. We discuss predicted quantities of the Euler-Heisenberg Lagrangian regarding vacuum birefringence that can be measured, such as the rotation of the polarization plane. Also, the cross section of elastic photon-photon scattering in the CoM system is given. We mention that axions could also induce a birefringence.

3.1 Effective field theory

In the previous section we mentioned that we are interested in LbyL interactions mediated via e^+e^- pairs since this phenomenon only involves the electromagnetic interaction. We defined this as QED LbyL scattering and we mentioned that the relevant parameter regime is one of low photon energy w.r.t. the electron mass. At photon energies of the order of the electron mass and higher we have to take into account additional virtual fermion pairs, such as $q\bar{q}$ pairs, that can mediate photonic interactions. At arbitrary photon CoM energies LbyL interactions are theoretically described by QFT. However, with our purpose of describing photonic interactions only via e^+e^- pairs, it is not useful to employ a complete QED treatment. In this chapter we discuss how photon-photon interactions are theoretically treated at photon energies far below the electron mass, the energy regime of importance to us. What happens at higher energies is not important for our purposes. This is where the idea of (quantum) effective field theory comes in. A field theory is called "effective" when it only describes the physics at a particular energy scale while forgetting about all the other Degrees of Freedom (DoFs) at higher energies. It is thus important to look at what the relevant energy scale (E) is of the physics in which we are interested. We are interested in low energy photon interactions. These energies correspond to the relevant energy scale E. Let's denote the higher energy scale related to the physics we want to describe by Λ. We want to study interactions between photons via e^+e^- pairs. The e^+e^- pairs are the irrelevant DoFs associated to the energy scale Λ since the electron mass of approximately 0.5 MeV

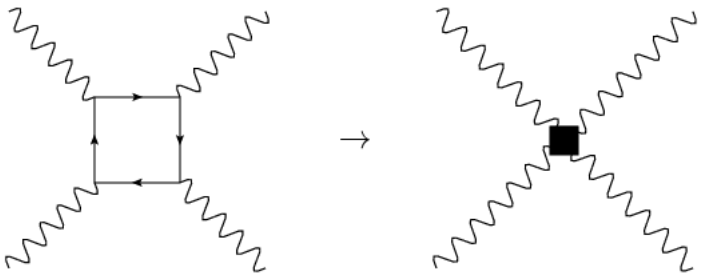

Figure 3.1: LbyL-scattering in QED (left) vs. LbyL-scattering in effective Euler-Heisenberg theory (right).

is much larger than the photon energies that we consider, at least theoretically[1]. We can therefore forget about the e^+e^- DoFs. This means we set $\Lambda = m_e$. To built a general effective field theory (EFT), an effective Lagrangian is built in terms of an expansion in the ratio of relevant and irrelevant energy scales $\frac{E}{m_e}$, respecting the underlying symmetries (Lorentz-symmetry and CPT-symmetry). This "forgetting" of the DoFs of electrons refers to the procedure of "integrating out" the Dirac Lagrangian from the QED Lagrangian. The one-loop vertex becomes an effective one-loop vertex (see figure 3.1). To be clear, in this effective picture the electrons and positrons did not disappear but they appear suppressed by terms proportional to $\frac{E_\gamma}{m_e}$. All other charged virtual fermion and boson loops are even more suppressed due to their (much) higher mass. This low energy effective Lagrangian is what is called the Euler-Heisenberg (EH) Lagrangian. For $E_\gamma \ll m_e$ its treatment of LbyL interactions is equivalent to a complete QED treatment. For photon energies approaching the electron mass and higher, a full QED treatment is necessary to describe LbyL scattering.

3.2 General remarks on NLEDs

Since the EH Lagrangian is a NLED we include some general remarks on this class of theories. The electromagnetic field equations for the vacuum, in any NLED, have the familiar form of the Maxwell equations in matter

$$\begin{aligned} \nabla \times \vec{H} = \frac{\partial \vec{D}}{\partial t}, \quad \nabla \cdot \vec{D} = 0 \\ \nabla \times \vec{E} = -\frac{\partial \vec{B}}{\partial t}, \quad \nabla \cdot \vec{B} = 0 \end{aligned} \tag{3.1}$$

but with the difference that $\vec{H}$ and $\vec{D}$ are of course non-linear in $\vec{E}$ and $\vec{B}$. These fields are respectively called the electric displacement field and the auxiliary field[2]. In different theories these fields depend differently on the electric and magnetic field,

[1] In chapter 4 the photons in the ATLAS experiment have CoM energies $E > 6$ GeV.

[2] It is confusing to call $\vec{H}$ the magnetic field. We follow the naming of David Griffiths in his textbook on classical electrodynamics [2].

since they are defined by the Lagrangian through the constitutive relations [8]

$$\vec{D} \equiv \frac{\partial \mathcal{L}}{\partial \vec{E}} \tag{3.2}$$

$$\vec{H} \equiv -\frac{\partial \mathcal{L}}{\partial \vec{B}} \tag{3.3}$$

We should also mention that any NLED can be written in terms of the Lorentz-invariants of classical electrodynamics. Recall the electromagnetic field tensor and its dual tensor from the beginning of chapter 2. In matrix representation, they are 4×4 antisymmetric matrices

$$F^{\mu\nu} = \begin{pmatrix} 0 & E_x & E_y & E_z \\ -E_x & 0 & B_z & -B_y \\ -E_y & -B_z & 0 & B_x \\ -E_z & B_y & -B_x & 0 \end{pmatrix}$$

and its dual tensor

$$\tilde{F}^{\mu\nu} = \begin{pmatrix} 0 & B_z & B_y & B_z \\ -B_x & 0 & -E_z & E_y \\ -B_y & E_z & 0 & -E_x \\ -B_z & -E_y & E_x & 0 \end{pmatrix}$$

The dual tensor can be directly obtained from the field tensor by substitution of $\vec{E} \to \vec{B}$ and $\vec{B} \to -\vec{E}$. This is a symmetry, or more precisely, a duality of the Maxwell equations in vacuum. Consequently, we can define the following Lorentz-invariants[3]

$$\mathcal{F} \equiv F_{\mu\nu}F^{\mu\nu} = -2(E^2 - B^2) \tag{3.4}$$

and

$$\mathcal{G} \equiv F_{\mu\nu}\tilde{F}^{\mu\nu} = -4(\vec{E} \cdot \vec{B}) \tag{3.5}$$

where 3.4 is a scalar while 3.5 is a pseudoscalar. This distinction will be important in the following analysis.

3.3 The Euler-Heisenberg Lagrangian

The QED Lagrangian reduces to the EH Lagrangian for low energy photons compared to the electron mass ($E_\gamma \ll m_e$). It describes all orders of one-loop photon-photon interaction processes mentioned in the previous chapter and vacuum pair-production effects. Hans Euler and Werner Heisenberg published the effective Lagrangian in the abstract of their paper from 1936 in a closed-form integral representation [20].

$$\mathcal{L} = \frac{e^2}{hc}\int_0^\infty \frac{d\eta}{\eta^3} e^{-\eta}\left\{ i\eta^2(\vec{E}\cdot\vec{B})\frac{\left[\cos(\frac{\eta}{E_c}\sqrt{E^2 - B^2 + 2i(\vec{E}\cdot\vec{B})}) + c.c.\right]}{\left[\cos(\frac{\eta}{E_c}\sqrt{E^2 - B^2 + 2i(\vec{E}\cdot\vec{B})}) - c.c.\right]} + E_c^2 + \frac{\eta^3}{3}(B^2 - E^2)\right\} \tag{3.6}$$

[3]Any NLED is formulated in terms of these Lorentz invariants. These are actually the only Lorentz invariant objects in classical electrodynamics.

Here E_c denotes the critical field strength. C.c. stands for the complex conjugate. This expression holds for energies far below the electron mass and field strengths up to the order of the critical field strenghts. Then, the integral no longer converges. The real part of this Lagrangian corresponds to all orders of photon-photon scattering in the one-loop approximation. The imaginary part is associated to the vacuum pair production probability. The derivation of this expression not discussed in this thesis. Within QED, this expression is derived from the one-loop effective action [13]. This expression can be simplified if we assume weak electric fields, i.e. far below the critical Schwinger field strength $E \ll E_c$ and then expand 3.6 in a power series in terms of the Lorentz-invariants 3.4 and 3.5. Note that this requirement on the electric field strength also implies that we require weak magnetic field strengths ($B \ll B_{crit}$) since the amplitudes of E and B are related via the speed of light. In the following analysis we restore the summation sign for clarity. A general effective Lagrangian has this structure

$$\mathcal{L}_{eff} = \mathcal{L}_{max} + \mathcal{L}_{NL} = \sum_{i=0}^{\infty}\sum_{j=0}^{\infty} c_{i,j}\mathcal{F}^i\mathcal{G}^j \tag{3.7}$$

where the term with indices *i=j=0* is defined to be zero. This result can be simplified further using another assumption about the vacuum. We postulate that the vacuum is CPT invariant, i.e. it is invariant under parity, charge conjugation and time reversal transformations. The result is that all terms with an odd index j vanish. To see why this is the case we take a closer look at the first few terms of the infinite sum

$$\sum_{i=0}^{\infty}\sum_{j=0}^{\infty} c_{i,j}\mathcal{F}^i\mathcal{G}^j = c_{0,1}\mathcal{G} + c_{1,1}\mathcal{F}\mathcal{G} + c_{1,0}\mathcal{F} + c_{2,0}\mathcal{F}^2 + c_{0,2}\mathcal{G}^2 + ...+ \tag{3.8}$$

The first and the second term are pseudoscalars while the other two are scalars. Pseudoscalars violate parity conservation since they pick up a minus sign under reflections. We can generalize this further to all odd *j*. The result (with the appropriate values of the constants) is called the EH Lagrangian.

$$\mathcal{L}_{EH} = \sum_{i=0}^{\infty}\sum_{j=0}^{\infty} c_{i,2j}\mathcal{F}^i\mathcal{G}^{2j} \tag{3.9}$$

For our purposes in this thesis, at least concerning the aim of formulating non-linear QED phenomena theoretically, the first non-linear correction will be good enough to do our calculations. In chapter 4 we will run into problems because we will meet magnetic fields strengths of the order of the critical magnetic field strength. Here the perturbative method breaks down. The non-linear contributions to the Lagrangian arise first at $\mathcal{O}(m_e^{-4})$ as we will see. To this order there are only two terms allowed by all symmetry considerations. This non-linear term corresponds to LbyL-scattering. Let us write down this first order correction:

$$\mathcal{L}_{EH} \approx -\frac{1}{4}F^{\mu\nu}F_{\mu\nu} + c_{2,0}(F^{\mu\nu}F_{\mu\nu})^2 + c_{2,2}(F^{\mu\nu}\tilde{F}_{\mu\nu})^2 \tag{3.10}$$

$$= -\frac{1}{4}F^{\mu\nu}F_{\mu\nu} + \frac{\alpha^2}{90m_e^4}\Big\{(F^{\mu\nu}F_{\mu\nu})^2 + \frac{7}{4}(F^{\mu\nu}\tilde{F}_{\mu\nu})^2\Big\} + \mathcal{O}(m_e^{-8}) \tag{3.11}$$

The first term is the familiar Maxwell Lagrangian. $\alpha \equiv \frac{e^2}{4\pi\epsilon_0\hbar c} \approx \frac{1}{137}$ (in SI units) is the fine-structure constant, which is actually not a real constant as we have seen but depends on the energy scale considered, although for $E_\gamma \ll m_e$ considered here it is constant. The prefactor m_e^{-4} appears on dimensional grounds and α^2 appears since this term couples four photons. The constants c_1 and c_2 (note that the notation of the constants slightly changed) have values $c_1 = \frac{1}{90}$ and $c_2 = \frac{7}{360}$. These are the dimensionless low energy constants and can be computed in QED. In the literature, the constants c_1 and c_2 are usually defined in natural, Heaviside-Lorentz (HL) units.

$$c_1 \equiv \frac{2\alpha^2}{45m_e^4}, \quad c_2 \equiv \frac{14\alpha^2}{45m_e^4} \tag{3.12}$$

Here are the constant factors resulting from the tensor products (see 3.4 and 3.5) between the brackets absorbed into the constants. We can redefine these constants in SI units (see appendix A)

$$c_1 = \frac{2\alpha^2\hbar^3\epsilon_0^2}{45m_e^4c^5}, \quad c_2 = 7c_1 \tag{3.13}$$

We converted these constants to SI units in anticipation of calculations in section 3.5.1. The factor of seven between the two constants characterizes the EH Lagrangian. We arrive at the final form of the EH Lagrangian, expanded to quartic order in the electron mass, by rewriting the tensor products using the identities 3.4 and 3.5.

$$\begin{aligned} \mathcal{L}_{EH} &= \frac{1}{2}(E^2 - B^2) + \frac{2\alpha^2}{45m_e^4}(E^2 - B^2)^2 + \frac{14\alpha^2}{45m_e^4}(\vec{E}\cdot\vec{B})^2 \\ &= \frac{1}{2}(E^2 - B^2) + \frac{2\alpha^2}{45m_e^4}\Big\{(E^2 - B^2)^2 + 7(\vec{E}\cdot\vec{B})^2\Big\} \end{aligned} \tag{3.14}$$

Or in SI units (see appendix A)

$$\mathcal{L}_{EH} = \frac{\epsilon_0}{2}(E^2 - c^2B^2) + \frac{2\alpha^2\hbar^3\epsilon_0^2}{45m_e^4c^5}\Big\{(E^2 - c^2B^2)^2 + 7c^2(\vec{E}\cdot\vec{B})^2\Big\} \tag{3.15}$$

Expression 3.14 is the most important expression in this thesis and needs to be well understood. This non-linear term originates from the coupling of four photons with energies $E_\gamma \ll m_e$ via virtual e^+e^- pairs. Expression 3.14 holds for weak fields, i.e. $E \ll E_c$ and $B \ll B_c$. Strictly speaking these terms only appear when the background field is uniform and constant with respect to the appropriate length and time scale. To a good approximation constant and uniform mean that the field strength does not vary over a Compton wavelength ($\lambda_c \approx 3.9 \times 10^{-11} cm$)[4]. We will proceed with calculating the modified Maxwell equations and modified wave equations in the vacuum.

[4]This value corresponds to the reduced Compton wavelength, i.e. the Compton wavelength in terms of $\hbar$.

3.4 Weak field corrections

All calculations in this section can be found in Appendix B. To compute the first order corrections to the Maxwell equations we need the EL equations for fields. The EH Lagrangian depends on the field A^μ so we have

$$\partial_\mu \frac{\partial \mathcal{L}_{EH}}{\partial(\partial_\mu A_\nu)} - \frac{\partial \mathcal{L}_{EH}}{\partial A_\nu} = \partial_\mu \frac{\partial \mathcal{L}_{EH}}{\partial F_{\mu\nu}} = 0 \tag{3.16}$$

This can be easily done using two derivative identities related to the Lorentz invariants 3.4 and 3.5

$$\frac{\partial \mathcal{F}}{\partial F_{\mu\nu}} = 2F^{\mu\nu}, \quad \frac{\partial \mathcal{G}}{\partial F_{\mu\nu}} = 2\tilde{F}^{\mu\nu} \tag{3.17}$$

Using the EL equation we obtain the following equations of motion

$$\partial_\mu F^{\mu\nu} = \frac{4\alpha^2}{45m_e^4}\partial_\mu\Big\{4(F_{\alpha\beta}F^{\alpha\beta})F^{\mu\nu} + 28(F_{\alpha\beta}\tilde{F}^{\alpha\beta})\tilde{F^{\mu\nu}}\Big\} \tag{3.18}$$

When neglecting the non-linear contribution ($\alpha \approx 0$), the RHS vanishes and we obtain the classical Maxwell equations. Note that only the law of Gauss and the law of Ampère have changed. Lets look how these equations have changed. Using the constitutive relations 3.2 we obtain, up to first order

$$\begin{aligned}\vec{D} &= \vec{E} + \frac{2\alpha^2}{45m_e^2}\Big\{4(E^2 - B^2)\vec{E} + 14(\vec{E}\cdot\vec{B})\vec{B}\Big\} \\ \vec{H} &= \vec{B} + \frac{2\alpha^2}{45m_e^4}\Big\{4(E^2 - B^2)\vec{B} - 14(\vec{E}\cdot\vec{B})\vec{E}\Big\}\end{aligned} \tag{3.19}$$

We observe that the corrections are cubic in the fields. Taking the divergence of the first equation and the curl of the second we get

$$\begin{aligned}\nabla\cdot\vec{D} = \nabla\cdot(\vec{E}+\vec{P}) = \nabla\cdot(\vec{E} + \frac{2\alpha^2}{45m_e^4}(4(E^2 - B^2)\vec{E}) + 14(\vec{E}\cdot\vec{B})\vec{B}) \\ \nabla\times\vec{H} = \nabla\times(\vec{B}-\vec{M}) = \nabla\times(\vec{B} - \frac{2\alpha^2}{45m_e^2}(4(E^2 - B^2)\vec{B} - 14(\vec{E}\cdot\vec{B})\vec{E})\end{aligned} \tag{3.20}$$

Following Euler and Kockel, we can identify a polarization and a magnetization of the vacuum

$$\begin{aligned}\vec{P}_{vac} &= \frac{2\alpha^2}{45m_e^4}(4(E^2 - B^2)\vec{E}) + 14(\vec{E}\cdot\vec{B})\vec{B}) \\ \vec{M}_{vac} &= \frac{2\alpha^2}{45m_e^2}(4(E^2 - B^2)\vec{B} - 14(\vec{E}\cdot\vec{B})\vec{E})\end{aligned} \tag{3.21}$$

Reformulating these equations in terms of the vacuum polarization and magnetization we get

$$\nabla\times\vec{E} = -\nabla\cdot\vec{P}_{vac}, \quad \nabla\times\vec{B} = \frac{\partial E}{\partial t} + \frac{\partial P_{vac}}{\partial t} + \nabla\times\vec{M}_{vac} \tag{3.22}$$

These expressions make it indeed clear that the vacuum has the properties of a medium. From the modified Maxwell equations it is possible to derive the modified

wave equations. In terms of the vacuum polarization and magnetization these change to

$$\begin{aligned} \Box\vec{E} &= -\frac{\partial^2\vec{P}_{vac}}{\partial t^2} + \nabla(\nabla\cdot\vec{P}_{vac}) + \frac{\partial}{\partial t}(\nabla\times\vec{M}_{vac}) \\ \Box\vec{B} &= \nabla\times(\nabla\times\vec{M}_{vac}) + \frac{\partial}{\partial t}(\nabla\times\vec{P}_{vac}) \end{aligned} \tag{3.23}$$

Here $\Box \equiv \frac{\partial^2}{\partial t^2} - \nabla^2$ denotes the D'Alembertian operator. The wave equations show that wave behaviour is modified in the quantum vacuum. There exists perturbative solutions to these equations.

3.5 Results from the EH-Lagrangian

In this section we discuss quantitative predictions of the EH Lagrangian: The rotation of the polarization plane through effective QED LbyL scattering and the cross section of photon-photon scattering at low and high CoM energies.

3.5.1 Vacuum birefringence

The goal of the analysis below is to express the Stokes parameters in terms of the constants of the EH Lagrangian (c_1 and c_2). To measure variations in the polarization properties of light one has to measure the Stokes parameters, which is possible since they are functions of intensities. We start our calculation from the values of the indices of refraction corresponding to the two mutual orthogonal linear polarization modes, $n_\perp$ and $n_\parallel$. For a complete derivation of $n_\perp$ and $n_\parallel$ the reader is referred to [25].

The following analysis holds for an electromagnetic plane wave travelling in the $\hat{z}$-direction in a constant and uniform external magnetic field. Furthermore, this analysis uses natural-HL-units. We can define a polarization vector before entering the magnetic field ($z = 0$)

$$\vec{e}(z=0) = E_0(\cos\theta\hat{x} + \sin\theta\hat{y})e^{-i\omega t} \tag{3.24}$$

where θ is the angle between the polarization vector and the magnetic field, ω the angular frequency and E_0 the amplitude. We can decompose $\vec{e}$ into a perpendicular and a parallel component w.r.t. the external magnetic field.

$$\begin{aligned} \vec{e} &\equiv \vec{e}_\perp + \vec{e}_\parallel \\ e_\perp &= E_0\sin\theta e^{i(k_\perp z-\omega t)} \\ e_\parallel &= E_0\cos\theta e^{i(k_\parallel z-\omega t)} \end{aligned} \tag{3.25}$$

The corresponding indices of refraction experienced are [25]

$$\begin{aligned} n_\parallel &= 1 + 4c_1B_{ext}^2 \\ n_\perp &= 1 + c_2B_{ext}^2 \\ \Delta n = n_\parallel - n_\perp &= \frac{2}{15}\frac{\alpha^2}{m_e^4}B_{ext}^2 \end{aligned} \tag{3.26}$$

Expressions 3.26 show that different polarization modes travel with different phase velocities showing that the vacuum is birefringent. Using $k_\perp = n_\perp \omega$ and $k_\parallel = n_\parallel \omega$ and the two indices of refraction we define a phase as

$$\delta \equiv (k_\perp - k_\parallel)z = (n_\perp - n_\parallel)\omega z = (4c_1 - c_2)\omega B_{ext}^2 z \tag{3.27}$$

Recall the polarization ellipse of figure 2.7. The ellipticity angle χ and orientation angle ψ can be expressed in terms of the amplitudes of the two polarization modes and the phase δ. We get [3]

$$\begin{aligned} \tan 2\psi &= \frac{2E_{0x}E_{0y}}{E_{0x}^2 - E_{0y}^2}\cos\delta \\ \sin 2\chi &= \frac{2E_{0x}E_{0y}}{E_{0x}^2 + E_{0y}^2}\sin\delta \end{aligned} \tag{3.28}$$

These polarization ellipse parameters can be completely written in trigonometric terms since $\tan\theta = \frac{E_{0x}}{E_{0y}}$. Then the expressions in 3.28 become [9]

$$\begin{aligned} \tan 2\psi &= \tan 2\theta \cos\delta \\ \sin 2\chi &= \sin 2\theta \sin\delta \end{aligned} \tag{3.29}$$

To proceed we assume that δ and χ are small, i.e. $\delta \ll 1 \rightarrow B_{ext}^2 z \ll \frac{1}{(4c_1 - c_2)\omega}$ for fixed ω and $\chi \ll 1$ such that we obtain

$$\begin{aligned} \sin 2\chi \approx 2\chi &\approx \delta \sin 2\theta \\ \tan 2\psi &\approx \tan 2\theta \end{aligned} \tag{3.30}$$

From the second equation we observe that $\psi \approx \theta$. Recall the definition of the Stokes parameters (expression 2.18). Using that χ is small, $\psi \approx \theta$ and using the definition of δ, the Stokes parameters become

$$\begin{aligned} I &= I_0 \\ Q &= I_0 \cos 2\chi \cos 2\psi \approx I_0 \cos 2\theta \\ U &= I_0 \cos 2\chi \sin 2\psi \approx I_0 \sin 2\theta \\ V &= I_0 \sin 2\chi \approx I_0 (4c_1 - c_2)\omega B_{ext}^2 z \sin 2\theta \end{aligned} \tag{3.31}$$

Consequently, the rotation of the polarization plane due to effective LbyL scattering is

$$\Delta\psi_{QED} = (4c_1 - c_2)\omega B_{ext}^2 L \tag{3.32}$$

where L is the distance travelled perpendicular to the magnetic field direction. Note that this expression requires $B^2 L$ to be much smaller than $\frac{1}{(4c_1 - c_2)\omega}$. In chapter 4 we determine the values for B for fixed ω and L.

3.5.2 Cross section of photon-photon scattering

From the EH-Lagrangian it is possible to compute the differential and total cross section for (real) elastic QED photon-photon scattering. In the low energy limit the differential cross section in the CoM frame is equal to [24]

$$\frac{d\sigma}{d\Omega} = \frac{139}{4\pi^2(90)^2}\alpha^4\left\{\frac{\omega}{m_e}\right\}^6\frac{(3+cos^2\theta)^2}{m_e^2}, \qquad \omega \ll m_e \tag{3.33}$$

here ω denotes the CoM energy of the initial photons and m_e the mass of the electron (positron) mediating the interaction. The total cross section in the CoM system is given by

$$\sigma = \frac{973}{10125\pi}\frac{\alpha^4}{m_e^2}\left\{\frac{\omega}{m_e}\right\}^6, \quad \omega \ll m_e \tag{3.34}$$

We do not perform the calculation here since it is beyond the scope of this thesis. The calculation is rather long and involves QFT methods. A complete QED derivation for expression 3.34 can be found in [6]. The cross section increases very rapidly when increasing the photon energy. It is important to keep in mind that for LbyL scattering via e^+e^- loops, we have to require that $\omega \ll m_e$, since this is required for the EH Lagrangian to be a valid theory. This means the cross section for this process is terribly small. The cross section is in this case suppressed by a factor $\frac{1}{m_e^8}$. To get a flavour of the magnitude of the cross section, for visible light the energy is approximately 1 eV, which can be considered small compared to m_e. Before we can plug the numbers in, the total cross section has to be expressed in SI units (see Appendix A). The result is

$$\sigma = \frac{973}{10125\pi}\alpha^4\left\{\frac{\hbar\omega}{m_ec^2}\right\}^6\left\{\frac{\hbar}{m_ec}\right\}^2 \qquad \hbar\omega \ll m_ec^2 \tag{3.35}$$

This corresponds to a cross section of $\sigma = 7\times10^{-70}m^2 = 7\times10^{-42}$b. For high photon energies the cross section drops with increasing CoM energy

$$\sigma = 4.7\alpha^4\left\{\frac{m_e}{\omega}\right\}^2 \quad ,\omega \gg m_e \tag{3.36}$$

All these results hold for unpolarized photons and fixed scattering angles. The energy spectrum of the cross section has a peak around threshold of e^- production [24]. Karplus and Neumann estimated the peak of the cross section at $\omega \approx 3m_e \approx 1.5$ MeV [23]. Here the cross section equals about 1.6×10^{-6}b. From figure 3.2 it can be seen that the cross section spans a huge range of orders of magnitude. To be clear, this cross section maximum does not correspond to the maximum cross section of QED LbyL scattering. While increasing the CoM energy, $q\bar{q}$ loops start dominating over the e^+e^- loops. For QED LbyL scattering we have to keep the CoM energy far below 0.5 MeV. This means that the cross section for QED LbyL scattering remains very small.

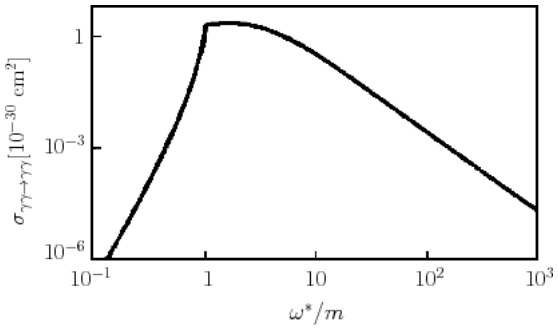

Figure 3.2: Energy spectrum of the total cross section of photon-photon scattering. ω^* denotes the center of mass energy. Note the peak at $\frac{\omega}{m} \approx 1$. This plot is taken from [6].

3.6 Axions and vacuum birefringence

We have seen that the axion is a hypothetical particle proposed to solve the so called strong CP-problem in QCD. In the presence of a strong magnetic field it is possible that a photon becomes an axion according to figure 3.3. The resulting axion can also induce a birefringence and dichroism of the vacuum. The axion can be a scalar or pseudoscalar particle. To account for contributions to the index of refraction of

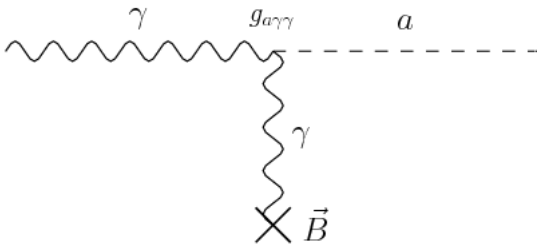

Figure 3.3: Illustration of axion-photon coupling. A photon interacting with a strong external magnetic field produces an axion, which can be a scalar or pseudoscalar particle. This figure is taken from [10].

the vacuum due to axions we have to add terms to the EH-Lagrangian. We get

$$\begin{aligned}\mathcal{L} = \frac{1}{2}(E^2 - B^2) + \frac{2\alpha^2}{45m_e^4}\Big\{(E^2 - B^2)^2 + 7(\vec{E}\cdot\vec{B})^2\Big\} + \frac{1}{2}\Big\{(\partial_\mu\phi)^2 - m_a^2\phi^2\Big\} \\ -\frac{G}{4}\phi\Big\{\delta_{a,s}(E^2 - B^2) + \delta_{a,p}(\vec{E}\cdot\vec{B})\Big\} \quad , a = s, p\end{aligned} \tag{3.37}$$

The third term between brackets is the familiar Klein-Gordon Lagrangian for the axion, which consist of a kinetic term and a mass term where m_a denotes the mass of the axion. The last term accounts for the coupling between axions and photons, where we have taken into account that an axion can be a scalar or a pseudoscalar particle. The δ symbol is the Kronecker delta. The label a is either equal to s (the axion is a scalar particle) or p (the axion is a pseudoscalar particle). —G— is a coupling constant. This time we obtain two equations of motion (one for the field $F_{\mu\nu}$ and one for the axion field ϕ). To derive the equation of motion w.r.t. $F_{\mu\nu}$ is

most easily done if the Lagrangian is rewritten in terms of the field tensor and then using the identities 3.17. The result are the previous equations of motion with an extra contribution of the axion-photon coupling:

$$\begin{aligned}\partial_\mu F^{\mu\nu} = \frac{4\alpha^2}{45m_e^4}\partial_\mu\Big\{4(F_{\alpha\beta}F^{\alpha\beta})F^{\mu\nu} + 28(F_{\alpha\beta}\tilde{F}^{\alpha\beta})\tilde{F^{\mu\nu}}\Big\} \\ -\frac{G}{2}\Big\{\delta_{a,s}F^{\mu\nu} + \delta_{a,p}\tilde{F}^{\mu\nu}\Big\}\partial_\mu\phi\end{aligned} \tag{3.38}$$

The equation of motion derived for ϕ is an inhomogeneous Klein-Gordon equation:

$$\Box\phi + m^2\phi = -\frac{G}{4}\Big\{\delta_{a,s}F^{\mu\nu}F_{\mu\nu} + \delta_{a,p}\tilde{F}^{\mu\nu}F_{\mu\nu}\Big\} \tag{3.39}$$

In appendix B a derivation is given of these equations of motion. Note that the existence of axions leads to a fifth Maxwell equation. For linear polarized light this gives contributions to the indices of refraction mentioned in section 3.5 in equation 3.26, depending on whether the axion is a scalar or pseudoscalar particle. Only one polarization mode will be modified. The contributions to the indices of refraction are

$$n_\parallel = -\delta_{a,s}\frac{G^2 I_0 m_a^2}{16\omega^2\omega_0^2 - m_a^4}, \quad n_\perp = -\delta_{a,p}\frac{G^2 I_0 m_a^2}{16\omega^2\omega_0^2 - m_a^4} \tag{3.40}$$

where the quantities with subscript 0 refer to background field properties and those without subscripts to the properties of the axion. In [32] a derivation is given of these indices of refraction.

Chapter 4

Measurements of non-linear QED effects?

We discuss recent measurements from [11, 29] which are claimed to be evidence for QED effects. We make comparisons with the theory to draw conclusions of the claims made in [11, 29].

4.1 Evidence for QED vacuum birefringence?

In this section we discuss optical polarimetric observations from the Very Large Telescope (VLT) at the ESO Cerro Paranal Observatory in Chile on the brightest member of the *Magnificent Seven* (M7) [29]. The observations are made by a collaboration of various astrophysical teams. The M7 are a group of radio-quiet isolated neutron stars (ISNs). The name of the brightest (and youngest) member of the M7 is RX J1856.5-3754. This collaboration studied the polarization properties of optical photons coming from the surface of this neutron star (NS). More specifically, they looked at the linear polarization degree (PD) and linear polarization position angle (PA) of the optical light. These observations are optical since they looked at wavelengths of $\lambda = 555.0$ nm, $\Delta\lambda = 61.6$ nm, which corresponds to energies of 2-2.5 eV. This corresponds to visible light.

The values they measured are: $P.D. = 16.43\% \pm 5.26\%$ and $P.A. = 145.39^\circ \pm 9.44^\circ$. They claim that the measured PD and PA provide evidence for the presence of vacuum polarization effects causing the vacuum to be birefringent, i.e. they claim that the observations are evidence for the box diagram of figure 4.1. Since the incoming photons have $E_\gamma \ll m_e$, they claim that these measurements are evidence for an interaction between a photon and a magnetic field via virtual e^+e^- pairs. This means it is claimed that evidence is observed for the LbyL interaction process predicted by Euler and Heisenberg, i.e. QED vacuum birefringence. If this is the case it would be the first observational evidence of QED effects in the strong field regime since the magnetic field of a NS is of the order $10^8 - 10^{10}$T, which is of the order of the critical magnetic field strength.

We will discuss if these particular values for the PD and PA are indeed evidence for QED vacuum birefringence.

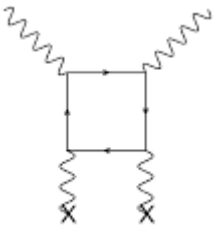

Figure 4.1: Illustration of the LbyL interaction responsible for vacuum birefringence. A photon interacts with an external magnetic field. At optical energies this loop consists of e^+e^- pairs.

4.1.1 Neutron stars and vacuum birefringence

Before going into the experiment and the discussion of the results we discuss the physical picture of the problem developed by Heyl and Shaviv [21]. It is known for some 30 years now that light emitted from surfaces of (neutron) stars with large magnetic fields (also known as *magnetars*) should be intrinsically polarized (orthogonal) to the magnetic field [28]. Magnetic fields of NSs vary from point to point on its surface. On each point the light is expected to be polarized orthogonal to the magnetic field direction. An observer on a distance will see effectively no net polarization in most cases due to the superposition of all the randomly oriented polarization vectors. In short, without considering vacuum polarization effects and any other effects that could influence the polarization, light would show no net (linear) polarization.

The orientation of the magnetic field changes slowly with increasing distance from the NS. When light travels away from the surface of the NS, the birefringence of the vacuum causes that the two polarization modes remain decoupled and orthogonal to the magnetic field direction. The polarization modes follow the direction of the magnetic field. It has to be said that this is only true if the magnetic field changes sufficiently slow. This is called the *adiabatic approximation*[1]. The further the light propagates away from the star, the more parallel the magnetic field orientations from the initial points on the surface become to each other. Since the polarization modes follow the magnetic field directions, they also become more and more parallel, until a region is reached where the magnetic field strength is well below the critical field strength and vacuum polarization effects are negligible. Consequently, the two polarization modes couple again. The value of the PD and PA depend on how long the polarization modes remain decoupled. This depends on the energy of the photons. This physical picture does not predict any specific values for the PA and PD. In principle, if every point of the NS surface is polarized orthogonal to the magnetic field, a value of 100% for the PD could be measured due to vacuum birefringence if the two polarization modes remain decoupled for the time necessary to reach this value. We see that QED effects could be a possibility to explain the non-zero measured values for the PD and PA.

[1]For a quantitative description for the conditions of the adiabatic approximation the reader is referred to [21].

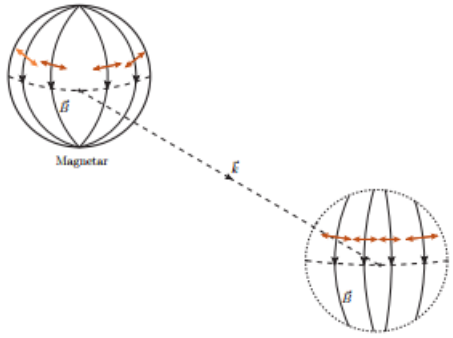

Figure 4.2: Illustration of the adiabatic approximation. The horizontal vectors are the photon polarizations which are orthogonal to the meradians (magnetic field lines). Since the magnetic field lines become more parallel, the polarization vectors also become more parallel since they adiabatically follow the changing magnetic field directions. This picture is taken from [26].

However, in the absence of QED effects and polarization contamination effects and when assuming that every surface point emits perfectly polarized light, a net polarization could be measured depending on the geometrical configuration of the magnetic field axis and the line connecting the point of emission on the surface of the star and the observer, i.e. the *observation line*. This configuration sets an upper bound on the measured PD which is approximated to be 40% according to [26], if the magnetic field lines are along the meradians as in figure 4.2. In the case of a dipole magnetic field geometry the geometric upper bound is about 20% according to [26]. These geometrical configurations require that the magnetic field axis and the observation line are orthogonal, which generally they aren't.

4.1.2 The experiment

The PA and PD are related to the (normalized) Stokes paratemers U and Q via relations 2.19 and 2.21:

$$\begin{aligned} P.A. &= \frac{1}{2}\tan^{-1}\left(\frac{P_U}{P_Q}\right) \\ P.D. &= \sqrt{P_Q^2 + P_U^2} \end{aligned} \tag{4.1}$$

To determine the Stokes parameters you have to measure intensities (photon fluxes), as we have mentioned before. Indeed, this is what they have done. Photon fluxes of the *ordinary* and *extraordinary* beams are measured at four different half-wave retarder plate angles α. The PA and PD of the optical light are calculated using various surface models as functions of two angles χ and ξ. ξ is called the *inclination angle*. It is the angle between the magnetic field axis and the axis of rotation. χ is the angle of the inclination of the line of sight w.r.t. to the magnetic field axis. In these various surface models[2] they compared calculations including vacuum polarization effects with those not containing vacuum polarization effects. The observed value

[2]Various surface emission models are used since the surface emission mechanism also influences the linear polarization.

of the PD was never reproduced in the models not containing vacuum polarization effects. Only values below the measured value were calculated.

4.1.3 Perturbative QED predictions

In the previous chapter we have calculated an expression for the angle of rotation of the polarization plane (expression 3.32) using the perturbative EH Lagrangian, i.e. we assumed that $B \ll B_{crit}$. In SI units (see appendix A) this expression becomes

$$\Delta\psi_{QED} = \frac{6\alpha^2\hbar^4\epsilon_0^2}{45m_e^4c^3e^2}\omega B^2 L \tag{4.2}$$

where ω is the angular frequency of the light, B the amplitude of the magnetic field of the NS and L the distance in which vacuum polarization effects can be considered relevant, i.e. the distance in which the magnetic field strength is of the order of the critical field strength. Regarding the use of the perturbative EH Lagrangian, in the optical regime the low energy condition $E_\gamma \ll m_e$ is satisfied. However, magnetic fields around NSs are of the order of the critical field strength. The weak field condition $B \ll B_{crit}$ is therefore not satisfied. This implies that difficulties will arise with perturbative methods in this regime. The perturbative expression for the rotation of the polarization plane above will therefore give not a clear prediction. To calculate $\Delta\psi_{QED}$ non-perturbative methods are necessary. This means we have to take into account all higher order processes in α, i.e. α^n with $n > 2$.

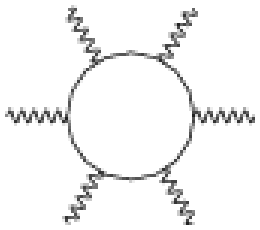

Figure 4.3: A α^3 process.

This yields a non-perturbative expression for $\Delta\psi_{QED}$. This is beyond the scope of this thesis.

To proceed, we can look at the results of perturbative calculations. If we naively assume that the magnetic field is constant we get answers that do not make sense. For $L = 10$Km (the typical radius of a NS), $B = 10^8T$ and $\omega = 3.1 \times 10^{15}$rad/s we get $\Delta\psi_{QED} \approx 10^5$rad. To produce something more useful we could take a closer look at the geometry of the magnetic field. It is known that the magnetic field strength drops very quickly with increasing distance from the center of the NS. According to [31], for a rotating NS, the amplitude $B \propto \frac{R_N^3}{r^3}$ where R_N is the radius of the NS and r the distance from the center of the star. Since $\Delta\psi_{QED}$ is proportional to B^2 we see that it drops as $\frac{1}{r^6}$, which is very fast.

To calculate $\Delta\psi_{QED}$ we have to integrate along the path of the photon. We assume the photons travel in the radial direction.

$$\Delta\psi_{QED} = \frac{6\alpha^2\hbar^4\epsilon_0^2}{45m_e^4c^3e^2}\omega|B|^2R_N^6\int_{R_N}^{\infty}\frac{1}{r^6}d\vec{r} = \frac{6\alpha^2\hbar^4\epsilon_0^2}{45m_e^4c^3e^2}\frac{\omega|B|^2R_N}{5} \tag{4.3}$$

This only yields an additional factor 0.2 and therefore the answer remains unsatisfying. With perturbative expression 4.2 we could produce any answer between 0 and 2π by varying B^2L. One could determine the perturbative regime by setting a bound on B^2L for fixed ω by requiring the α^2 term in the perturbative expansion to be $\ll 1$

$$\begin{gathered}\Delta\psi_{QED} = 1 + \alpha^2\Big\{\frac{6\hbar^4\epsilon_0^2}{45m_e^4c^3e^2}\omega B^2L\Big\} + ..., \qquad \alpha^2\frac{6\hbar^4\epsilon_0^2}{45m_e^4c^3e^2}\omega B^2L \ll 1rad \\ B^2L \ll 2\times 10^{15}Tm\end{gathered} \tag{4.4}$$

For L=10^4m we must require B$\ll 10^6$T.

We have also discussed axions in the context of vacuum birefringence. According to [26] axion-photon coupling could cause a transition between the two orthogonal polarization modes. The orthogonal polarization mode can switch to the parallel mode and vice versa. This effect becomes important at low photon energies (on the order of 0.1 eV). However, the NS cannot be observed at this energy because it is too faint [26]. In the optical regime no significant change of the linear polarization is expected. In addition, for this jump between polarization modes, the axion-photon coupling strength must be of the order $|G| \approx 10^{-7}GeV^{-1}$[26], which has already been excluded [19].

4.1.4 Concluding remarks

Pertubative EH theory does not make specific predictions for $\Delta\psi_{QED}$ since the weak field condition is not satisfied. Any PA, and therefore any PD, can be found by varying B^2L. We have seen that it is believed that the polarization vectors follow the magnetic field direction in the region where vacuum birefringence effects are significant, which in principle could yield a PD of 100%. The fact that a non-zero $\Delta\psi$ is measured could be interpreted as a confirmation of the theory. However, there are statistical and geometrical objections to this claim [26]. Even in the absence of QED vacuum birefringence, in the most favourable geometric configuration for the magnetic field, i.e. $\chi = \pi$ and $\xi = 0$, a value around 16% could possibly be obtained. The error in the PA is more than 5 standard deviations away from zero, which seems strong evidence. But the PD is only 3 standard deviations away from zero, which is less convincing. A 3σ effect is far from strong evidence for the existence of vacuum birefringence.

A more elaborate statistical analysis can be found in [26]. They have studied how likely it is that non-zero values for the PD are obtained in models with and without vacuum birefringence. This is done by calculating the *Bayes factor* or *likelihood* L. This Bayes factor appears to be greater than 1 when using the data mentioned at the beginning of this chapter, which means the measured data favors the absence

of vacuum birefringence. Consequently, a lower bound on the PD of approximately 22% is found[3]. It follows that PD values larger than approximately 30% would be strong evidence for vacuum birefringence effects[4] with the present statistics.

It could be that the physical picture is wrong. This would imply that light from a NS is not at every point intrinsically polarized. Then, a measurement of 16% could be a maximum PD due to QED effects. However, non-perturbative calculations have to be made to make sure which PD values are characteristic of vacuum QED effects. Furthermore, this would contradict 30 years of astrophysical literature on this subject.

To summarize, non-perturbative calculations, which means taking into account all higher order processes in α, have to be made to specify which PA and PD are really characteristic for vacuum polarization effects in the optical regime at critical magnetic fiels. The measured values of the PA and PD seem too low to be evidence for vacuum birefringence. A reduction of the error in the PD reduces the value for the PD necessary for a Bayes factor of 0.01, i.e. better statistics lead to stronger evidence for QED vacuum birefringence.

[3]This corresponds to a Bayes factor of 1.
[4]This corresponds to a Bayes factor of 0.01.

4.2 Real QED Light-by-light scattering at the LHC?

The ATLAS collaboration at CERN claimes that evidence for LbyL scattering is observed at the LHC [11]. We discuss whether this is the case and if so, which type of LbyL scattering is observed. This means we will look at which fermions could possibly form the loop and if the photons involved in the interaction are on-shell or not. Furthermore, we will discuss the physical principles of the experiment. We will not go into the complete experimental setup, background effects and details of the event selection procedure.

4.2.1 The experiment

The ATLAS collaboration studied LbyL-scattering using ultra-relativistic heavy-ion collisions. Heavy ions consist of a lot of quarks, which interact via the strong interaction. At distances of the order of 1 fm, the strong force dominates over the other fundamental forces. Studying LbyL scattering involves the electromagnetic interaction. What ATLAS did is that these collisions are *ultra-peripheral*, meaning that the perpendicular distance from the path of an object to the center of potential created by an approaching object is larger than the diameter of the object. This perpendicular distance is called the impact parameter, denoted by b. ATLAS used lead nuclei (Pb), which have atomic number $A = 208$ and a diameter of approximately 6 fm. This means the impact parameter $b > 12$ fm. In this case the strong interaction can be neglected in favour of the electromagnetic interaction. A more precise value of b is not mentioned in [11].

The electromagnetic field strength of relativistic charged particles scales with the atomic number. In the case of a Pb nucleus, the electric field generated is much stronger than the critical Schwinger field strength (about 7 orders of magnitude, the electric field generated is of the order 10^{25} V/m). Ultra-relativistic charged particles can be described by the equivalent photon approximation (EPA) [18]. Figure 4.4 gives an illustration of this approximation. The electromagnetic fields of the nuclei can be treated as photon-beams in this approximation. The electromagnetic interaction between the lead nuclei can then be described as the exchange of two *quasi-real* photons. These photons could scatter off each other according to the one-loop diagram. Whether this happens via one loop depends on the CoM energy. The crucial measurement is then the detection of two photons [5]. Pb-nuclei are used because the photon flux scales as Z^2, so that a large cross section can be obtained. The Pb nuclei leave via the LHC beam-pipe, so that the expected signature is only two photons. The Pb nuclei remain intact after the interaction so this means that this collision is elastic.

[5] The complete reaction is $Pb + Pb\gamma^*\gamma^* \to Pb^* + Pb^*\gamma\gamma$.

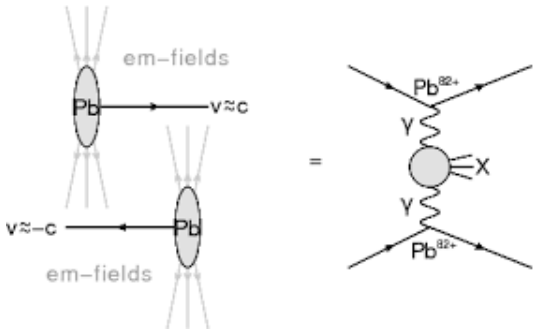

Figure 4.4: Illustration of the EPA. This figure is taken from [11].

Claimed results

The fact that the initial photons are "quasi-real" does not mean that detection of real LbyL scattering is completely excluded. It is possible that there is a small contribution of the real photon-photon scattering process. The virtuality or 'off-shellness' Q^2 of the initial photons is less than the inverse square of the radius of the charge distribution. For this experiment Pb-nuclei are used, which have a charge radius of approximately 6 fm. This gives a virtuality of $Q^2 < 10^{-3} GeV^2$. But ATLAS also did not claim to have seen real LbyL scattering. The process that ATLAS claimes to have seen is LbyL scattering of two quasi-real photons via a fermion loop, resulting in two real photons. In the next section we will mention the requirement for calling a photon 'quasi-real'. ATLAS found the diphoton invariant mass spectrum of figure

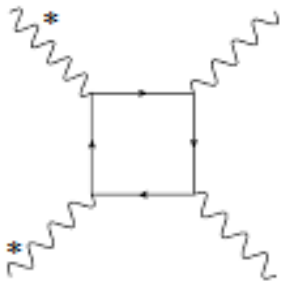

Figure 4.5: Two quasi-real photons, denoted by a "*", scatter with each other via a fermion loop, yielding two on-shell photons.

4.6. The red histogram shows the Monte-Carlo (MC) simulation of the $\gamma\gamma \to \gamma\gamma$ process. It tells us the number of LbyL scattering events within a specific diphoton invariant mass interval. The MC simulation generates events by taking into account charged lepton loops and quark loops. The blue and grey histograms show the MC simulations of background effects which we are not going to discuss. The points show the obtained data. The vertical bars are the statistical uncertainties in the amount of detected events. The spectrum shows that the data agrees with the MC simulation for LbyL scattering. This would mean that ATLAS detects a continuum of quasi-real LbyL scattering processes. However, we observe that the data point around 10 GeV is above the MC simulation. We will come back to this,

since this opens the possibility of an interruption of the continuum by the creation of a hadronic resonance state. The question we try to answer is whether it is really

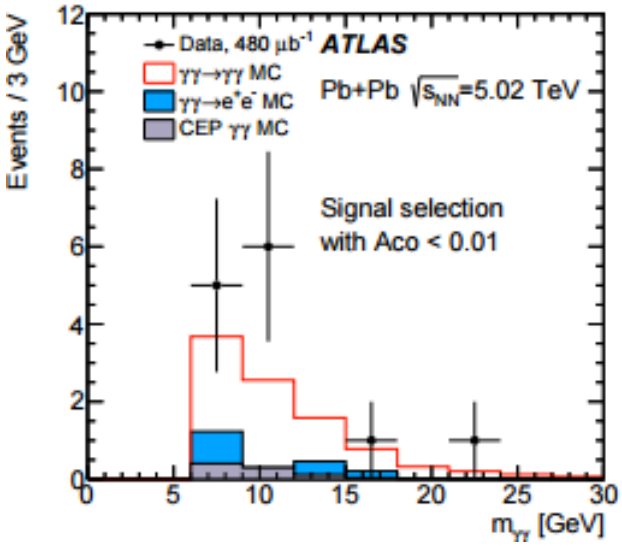

Figure 4.6: Diphoton invariant mass spectrum measured by ATLAS. The number of events per 3 GeV versus diphoton invariant mass in GeV. As can be seen from the horizontal axis, they detected events in an energy range of 6 GeV $< m_{\gamma\gamma} <$ 30 GeV.

the process of figure 4.5 that is detected and if so, what type of LbyL scattering this is. This requires some relativistic kinematics, which we are going to discuss now.

4.2.2 Relativistic kinematics

In special relativity the CoM energy is measured by the quantity s which is called a *Mandelstam variable*. Using relativistic kinematics (conservation of four-momentum), with q_i (i=1,2) the four-momentum of the initial photons and assuming the photons are on-shell ($q_i^2 \equiv m^2 = 0$), we see that

$$s = (q_1 + q_2)^2 = 2q_1q_2 = 2(E_1E_2 - \vec{p}_1 \cdot \vec{p}_2) = 2(E_1E_2 - |p_1||p_2|\cos\theta) \tag{4.5}$$

where θ is the scattering angle between the photons. It is important to note that the initial photons can have invariant masses equal to zero (they are on-shell), while still creating high energy/heavy particles/pairs. When the photons interact at $\theta = \pi$ (they collide head-on), which is actually a valid approximation at velocities near the speed of light of the Pb nuclei, the final invariant mass is maximum and becomes

$$s = 4E_1E_2 \tag{4.6}$$

where we used that $E_i = |p_i|$ for on-shell photons. The CoM energy is therefore equal to

$$\sqrt{s} \equiv m_{\gamma\gamma} = 2\sqrt{E_1E_2} > 6GeV \tag{4.7}$$

where $m_{\gamma\gamma}$ denotes the diphoton invariant mass. Recall that QED LbyL scattering requires CoM energies far below the electron mass, i.e. $\sqrt{s} \ll 0.5$ MeV. It is obvious

that detection of this process is excluded in this experiment. At the energies of ATLAS, virtual $q\bar{q}$ pairs dominate over virtual e^+e^- pairs. This implies that if ATLAS really detected the loop diagram in figure 4.5, then its loop consists of $q\bar{q}$ pairs, which means they detected quasi-real QCD LbyL scattering. We can exclude virtual bosonic loops consisting of W-bosons since these become only important at diphoton invariant masses greater than twice the invariant mass of a W-boson, which is way beyond the energy range where ATLAS is interested in (see figure 4.6). For quasi-real LbyL scattering we have to require that

$$\frac{Q^2}{s} \ll 1 \tag{4.8}$$

For $s > 36GeV^2$ and $Q^2 < 10^{-3}GeV^2$ this is the case. We get, in this 'worst case scenario' (largest Q^2 and lowest s):

$$\frac{Q^2}{s} \approx \frac{10^{-3}}{36} \approx 3 \times 10^{-5} \ll 1 \tag{4.9}$$

For clarity we include here an overview of the requirements on Q and s when to call a photon virtual, quasi-real or real.

$$\begin{aligned} Q^2 = 0 \quad &\rightarrow \quad real = on - shell \\ \frac{Q^2}{s} \ll 1 \quad &\rightarrow \quad quasi - real = off - shell \\ \frac{Q^2}{s} \geq 1 \quad &\rightarrow \quad virtual = off - shell \end{aligned} \tag{4.10}$$

Note that low energy experiments are not necessarily a better approach to real LbyL scattering. The smaller the ratio of 4.8, the better the approximation of real LbyL scattering. What we have seen up to now is that we have excluded real and virtual QED LbyL scattering, leaving quasi-real QCD LbyL scattering as the claimed detected process by ATLAS.

4.2.3 Diphoton measurements

Since the requirement of $\frac{Q^2}{s} \ll 1$ is satisfied and the detected signal agrees with the MC simulation for LbyL scattering, it seems that ATLAS detects a continuum of quasi-real QCD LbyL scattering. We already mentioned the possibility of the creation of a hadronic resonance state around 10 GeV. We want to discuss this now in more detail. In this context we also want to discuss the Crystall Ball (CB) experiment.

Despite the low values of the four-momenta (q_1 and q_2) of the photons, $\sqrt{s}$ can be very large, which in fact is the case (see equation 4.7). Recall the process of the production of hadronic resonances from chapter 2. Two photons produce an intermediate bound quarkonium state (if $\sqrt{s}$ is large enough) which could decay into two photons if its spin is not equal to 1 according to the Landau-Yang theorem. Consequently, in the diphoton invariant mass spectrum there is a peak at a certain value, corresponding to the invariant mass of the intermediate resonance state. Hence the name "hadronic resonance". Below 4 GeV, diphoton decay could originate from

$u\bar{u}$, $d\bar{d}$, $s\bar{s}$ and $c\bar{c}$ resonance states with spin not equal to one. However, since ATLAS starts detecting photons from diphoton invariant masses of 6 GeV, diphoton detection of diphoton decay of the above mentioned resonance states is highly suppressed. Diphoton invariant masses of 6 GeV $< m_{\gamma\gamma} <$ 30 GeV, which is the invariant mass interval of ATLAS, still allow for particular production of hadronic resonances. In this energy range bottomonium ($b\bar{b}$) resonance states are produced. We have to consider the $b\bar{b}$ resonances with spin equal to zero and two. These are the $\chi_{b,0}$ and $\chi_{b,2}$ (they have J=0,2 respectively) $b\bar{b}$ resonance states. They are allowed to decay into two photons. They have masses of 9.86 GeV and 9.91 GeV respectively.

Coming back to the earlier mentioned data point around 10 GeV in figure 4.6, this data point could be due to the diphoton decay of $\chi_{b,0}$ and $\chi_{b,2}$. This data point lies above the MC simulation and therefore it is possible to explain this measurement at this particular diphoton invariant mass by $\chi_{b,0}$ and $\chi_{b,2}$ diphoton decay. Better statistics around the invariant masses of $\chi_{b,0}$ and $\chi_{b,2}$ are needed to really draw conclusions about this data point. Diphoton decay of hadronic resonances, such as the η, η' and π^0, have been observed many times earlier in e^+e^- collision experiments, for instance in the CB experiment [33]. In 1988 the CB collaboration did an experiment in which they tested the reaction $e^+e^-(\gamma^*\gamma^*) \rightarrow e^+e^-(\gamma\gamma)$. The purpose of the CB experiment was to study simultaneous pseudoscalar (π^0, η and $\eta^{'}$) formation in the energy range 100-3000 MeV. In the context of the creation $q\bar{q}$ resonances in particle collisions, the possible production of $\chi_{b0,b2}$ resonances by ATLAS is new since these are $b\bar{b}$ states. The physical process of the production of $b\bar{b}$ resonances is not new, it is a higher energy version of the CB experiment and the e^+e^- pairs are replaced by Pb-nuclei. To conclude whether ATLAS or CB did a better job concerning quasi-real (QCD) LbyL scattering, we have to look which ratio of $\frac{Q^2}{s}$ is the smallest. In the CB experiment the initial photons have virtuality $Q^2 \approx 10^{-5} GeV^2 = 10 MeV^2$. This is two orders of magnitude below the virtuality of the photons of ATLAS. However, in this case we have in the worst case scenerio:

$$\frac{Q^2}{s} \approx \frac{10^{-5}}{m_{\pi^0}^2} \approx \frac{10^{-5}}{(0.14)^2} \approx 5 \times 10^{-4} \tag{4.11}$$

This value is one order of magnitude larger than the value which ATLAS reaches. Therefore, regarding the purposes of quasi-real (QCD) LbyL scattering, ATLAS did a better job.

4.2.4 Concluding remarks

The experiment done by ATLAS provides evidence for quasi-real QCD LbyL scattering with the possibility of the creation of $\chi_{b0,b2}$ resonance states. It is certainly not evidence for real QED LbyL scattering since $\sqrt{s} \gg m_e$ and $Q^2 \neq 0$. As we already mentioned, better statistics are needed in the region of 10 GeV to make sure whether the detected photons are coming from a direct scattering process between two incoming quasi-real photons. With the current statistical data, it cannot be excluded that the diphoton detection originates from $\chi_{b0,b2}$ decay. The ATLAS experiment was not designed to look for (real) QED LbyL scattering, they where looking for quasi-real QCD LbyL scattering. We want to conclude with remarks on particle collision experiments.

Remarks on particle collision experiments

We mentioned earlier that particle accelerators have studied the high energy regime extensively but not the low energy regime. This can also be seen in following figure. At CoM energies below a few 100 MeV in e^+e^- collisions there is not yet data known.

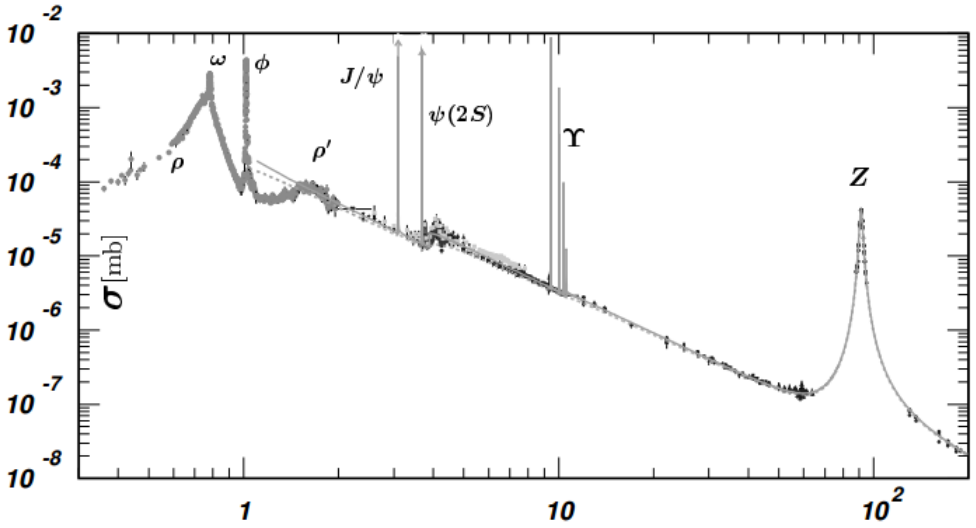

Figure 4.7: A plot of the cross section σ in mb ($= 10^{-3}$b) versus CoM energy ($\sqrt{s}$) in GeV in e^+e^- collisions.

It could be that new resonances can be found at low CoM energies via photon fusion processes. Also, around photon CoM energies of $E_\gamma \approx 3m_e \approx 1.5$ MeV, the cross section for photon-photon scattering attains a maximum of 1.6×10^{-6}b (see figure 3.2). It seems that low energy e^+e^- collision experiments may reveal new particles and it increases the cross-section for direct detection of off-shell QCD LbyL scattering. In this case $\sqrt{s}$ is small but $\frac{Q^2}{s}$ can still be large. Hence, we refer here to "off-shell" QCD LbyL scattering, since the photons can be either virtual or quasi-real. Colliding laser beams, with typical energies of several eV, could be an option to create even more on-shell QED LbyL scattering events compared to particle collision experiments. The price to pay is that in this case the cross section is so terribly small compared to the maximum of 1.6×10^{-6}b in figure 3.2. In addition, at low energies the photons remain off-shell. To approach real LbyL scattering, the

virtuality has to be minimized compared to the energy in the CoM system. This means we do not necessarily have to perform low energy experiments to test (almost real) LbyL scattering and the low value of the cross section is no longer a problem. However, the unfortunate conclusion is that it seems impossible to create perfectly real photons. Detection of real LbyL scattering is beyond the current experimental capabilities.

A consolation

Despite not observing real QED/QCD LbyL scattering directly, there is no reason to have doubts about whether the one-loop process where either e^+e^-, $q\bar{q}$ or W-boson pairs mediate the photon interaction occurs. As already briefly mentioned in chapter 2, measurements of the anomalous magnetic moment of the muon and the electron prove the correctness of the e^+e^- loop contribution. Also, the contribution of the box diagram is observed in Delbrück scattering and photon splitting experiments. But unfortunately, this is all indirect evidence for LbyL interactions and therefore for fluctuations in the vacuum energy. The detection of quasi-real ($\frac{Q^2}{s} \ll 1$) QCD LbyL scattering at $\sqrt{s} \gg m_e$ by ATLAS is direct evidence for LbyL scattering and therefore for vacuum fluctuations. Furthermore, there is no reason to doubt that in the limit $Q^2 \to 0$ and for $\sqrt{s} \ll m_e$ photons also scatter. Nevertheless, it is important that experimental physics strives to observe real QED LbyL scattering directly, since its this process that has to be compared to classical electrodynamics. This would prove a fundamental difference between QED and classical electrodynamics. In addition, it would be direct evidence of fluctuations in the zero-point-energy.

Chapter 5

Conclusions

We have seen that the low energy effective field theory of Euler and Heisenberg contains a lot of physics. Its prediction on the possibility of photon-photon interactions has been proven right in many experiments. Still, the fundamental QED process of real LbyL scattering via e^+e^- loops predicted by Euler and Heisenberg remains unobserved and one could ask the question if this is even possible to detect, though there is no reason to have doubts whether it occurs. There is indirect evidence for QED LbyL scattering and there are no physical reasons that in the limit $Q^2 \to 0$ the scattering process would not occur. The diphoton measurements of ATLAS are direct evidence for quasi-real QCD LbyL scattering. The statistics in the interval of 10 GeV in the diphoton invariant mass spectrum have to be improved in order to draw conclusions on the possibility of $\chi_{b,0}$ and $\chi_{b,2}$ diphoton decay. For off-shell QCD LbyL scattering (via $u\bar{u}$ or $d\bar{d}$), low energies on the MeV-scale are required to optimize the cross section according to figure 3.2. In addition, according to figure 4.7, new particles could be found in this energy regime. Experimentally, it seems not possible to create real LbyL scattering events since it is not known how to create the initial photons perfectly on-shell. The best approach to real QCD LbyL scattering events is to minimize the virtuality with respect to the CoM energy.

The non-zero measurements on the PA and PD of optical light from the ISN RX J1856.5-3754 could be explained through QED effects. However, the PD and PA seem too low to be evidence for QED vacuum birefringence. Based on statistical analyses using the current statistical data from [29], a PD of 30% would be strong evidence for vacuum birefringence. We could not verify the measured values in perturbation theory because of the extremely large field strengths around NSs. In perturbation theory, any value for the PA between 0 and 2π can be obtained by variation of B^2L. To make better quantitative predictions of values of the PA and PD in the optical regime, we have to take into account all higher order processes in α. This yields a non-perturbative expression for $\Delta\psi$. This could be a topic for further research. A reduction of the experimental error would be of great interest. Consequently, this could potentially be the first solid evidence for direct detection of a QED LbyL interaction via e^+e^- loops and provide evidence for fluctuations in the vacuum energy.

For now, we are left with the conclusion that both observations discussed in this thesis are not evidence for non-linear QED effects.

Appendix A

Dimensional analysis

We have converted a couple of times Heaviside-Lorentz (HL) ($\epsilon_0 = \mu_0 = 1$) units together with natural units ($\hbar = c = 1$) to SI units. We have done this in the case of the constants in the EH Lagrangian, the photon-photon scattering cross section (σ) and the angle of rotation of the polarization plane (ψ). All SI units can be expressed in mass (kg), length (m), time (s) and charge (C) dimensions. This means that units like Joules, Volts and Teslas are all derived from these dimensions. Let's define all these derived units in basic SI. We will also define the fundamental constants in SI units. We will need this in the following calculations.

$$\begin{gathered} 1[T] = 1\frac{kg}{As^2} \quad , 1[J] = 1\frac{kgm^2}{s^2} \quad , 1[V] = 1\frac{kgm^2}{As^3} \quad , 1[A] = 1\frac{C}{s} \\ [\hbar] = \frac{kgm^2}{s} \quad , [\epsilon_0] = \frac{A^2s^4}{kgm^3} \quad , [\mu_0] = \frac{kgm}{s^2A^2} \quad , [c] = \frac{m}{s} \quad , [e] = C \end{gathered} \tag{A.1}$$

In these units the fundamental constants have the following values

$$\begin{gathered} \hbar = 1.05 \times 10^{-34}\frac{kgm^2}{s} \quad , \epsilon_0 = 8.85 \times 10^{-12}\frac{A^2s^4}{kgm^3} \quad , \mu_0 = 4\pi \times 10^{-7}\frac{kgm}{s^2A^2} \\ c = 3.0 \times 10^8\frac{m}{s} \quad , e = 1.60 \times 10^{-19}C \end{gathered} \tag{A.2}$$

EH Lagrangian

Let's start with the constants in the EH Lagrangian. In HL and $\hbar = c = 1$ units the EH constants equal

$$\begin{gathered} c_1 = \frac{2\alpha^2}{45m_e^4} \quad , c_2 = \frac{14\alpha^2}{45m_e^4} \\ \alpha = \frac{e^2}{4\pi} \end{gathered} \tag{A.3}$$

The EH Lagrangian density in natural-HL units is

$$\mathcal{L} = \frac{1}{2}(E^2 - B^2) + \frac{2\alpha^2}{45m_e^4}(E^2 - B^2)^2 + \frac{14\alpha^2}{45m_e^4}(\vec{E} \cdot \vec{B})^2 \tag{A.4}$$

To begin with, we have to derive the units of the Lagrangian density. This can be derived from the definition of the action.

$$\begin{gathered} [S] = [\int dtd^3x\mathcal{L}] = [\hbar] = Js \\ [\mathcal{L}] = \frac{J}{m^3} = \frac{kg}{s^2m} \end{gathered} \tag{A.5}$$

In HL and $\hbar = c = 1$ units the EH constants have units

$$[c_1] = [c_2] = \frac{1}{kg^4} \tag{A.6}$$

To match with the Lagrangian density in SI units we have to equate the following terms

$$\begin{gathered}[\mathcal{L}] = [\gamma][c_1][B^4] \\ \frac{kg}{s^2 m} = [\gamma]\frac{1}{kg^4}\frac{kg^4}{A^4 s^8} = [\gamma]\frac{1}{A^4 s^8}\end{gathered} \tag{A.7}$$

Which means that the dimensions of γ equal

$$[\gamma] = \frac{kgA^4 s^6}{m} \tag{A.8}$$

γ is a quantity composed of powers of the fundamental constants ϵ_0, μ_0, $\hbar$ and c. It is important to realize that any combination of kilograms, seconds, meters and amperes can be uniquely expressed in terms of the these fundamental constants. In general, γ has the following structure

$$\gamma = \epsilon_0^\alpha \mu_0^\beta \hbar^m c^n \tag{A.9}$$

where α, β, m and n $\in \mathbb{Z}$. Substituting the dimensions of these constants in this expression we can derive the general dimensional structure of γ

$$[\gamma] = \left\{\frac{kg^{\beta+m}}{kg^\alpha}\right\}\left\{\frac{m^{2m+n+\beta}}{m^{3\alpha}}\right\}\left\{\frac{A^{2\alpha}}{A^{2\beta}}\right\}\left\{\frac{s^{4\alpha}}{s^{2\beta+m+n}}\right\} \tag{A.10}$$

Regarding equation A.8, we can derive a system of four linear equations in α, β, m and n. These are

$$\begin{gathered}\beta - \alpha + m = 1 \\ 2m + n + \beta - \alpha = -1 \\ 2\alpha - 2\beta = 4 \\ 4\alpha - n - m - 2\beta = 6\end{gathered} \tag{A.11}$$

A solution is $\alpha = 2$, $\beta = 0$, m=3 and n=-1. This means that

$$\gamma = \frac{\hbar^3 \epsilon_0^2}{c} \tag{A.12}$$

This means that $\gamma c_1 B^4$ has the same dimensions as the Lagrangian density in SI units. We can perform the same analysis for the term

$$[\mathcal{L}] = [\gamma][c_1][E^4] \tag{A.13}$$

Substituting the SI units for each term gives

$$\begin{gathered}\frac{kg}{s^2 m} = [\gamma]\frac{m^4}{A^4 s^{12}} \\ [\gamma] = \frac{kgs^{10}A^4}{m^5}\end{gathered} \tag{A.14}$$

This gives four linear equations

$$\begin{gathered}\beta-\alpha+m=1\\ 2m+n+\beta-3\alpha=-5\\ 2\alpha-2\beta=4\\ 4\alpha-n-m-2\beta=10\end{gathered} \tag{A.15}$$

A solution is $\alpha=2,\beta=0$, $m=3$ and $n=-5$. Thus, $\gamma=\frac{\hbar^3\epsilon_0^2}{c^5}$. The last term we have to fix is

$$[\mathcal{L}]=[\gamma][c_2][E^2][B^2] \tag{A.16}$$

This gives

$$[\gamma]=\frac{kgA^4s^8}{m^3} \tag{A.17}$$

We get again four linear equations. The solution is $\alpha=2,\beta=0,m=3$ and $n=-3$, giving $\gamma=\frac{\hbar^3\epsilon_0^2}{c^3}$. Actually, we should also convert the Maxwell Lagrangian to SI units (the first term of the EH Lagrangian).

$$\begin{gathered}[\mathcal{L}]=[\gamma_1][E^2]\quad and\quad [\mathcal{L}]=[\gamma_2][B^2]\\ \gamma_1=\epsilon_0\quad \gamma_2=\epsilon_0c^2\end{gathered} \tag{A.18}$$

This allows to define the EH Lagrangian in SI units. We get

$$\begin{aligned}\mathcal{L}&=\frac{\epsilon_0}{2}(E^2-c^2B^2)+\frac{2\alpha^2\hbar^3\epsilon_0^2}{45m_e^4c^5}(E^2-c^2B^2)^2+\frac{14\alpha^2\hbar^3\epsilon_0^2}{45m_e^4c^3}(\vec{E}\cdot\vec{B})^2\\ &=\frac{\epsilon_0}{2}(E^2-c^2B^2)+\frac{2\alpha^2\hbar^3\epsilon_0^2}{45m_e^4c^5}((E^2-c^2B^2)^2+7c^2(\vec{E}\cdot\vec{B})^2)\end{aligned} \tag{A.19}$$

which is the desired result. Consequently, we can define c_1 and c_2 in SI units as follows

$$c_1=\frac{2\alpha^2\hbar^3\epsilon_0^2}{45m_e^4c^5}\quad ,c_2=7c_1 \tag{A.20}$$

Cross section

The cross section of photon-photon scattering in SI units is easier to derive since this expression does not contain charge dimensions. In SI units the cross section has units of m^2

$$\begin{gathered}[\sigma]=[\gamma]\frac{[\omega^6]}{[m^8]}\\ m^2=[\gamma]\frac{1}{kg^8s^6}\\ [\gamma]=kg^8m^2s^6\end{gathered} \tag{A.21}$$

γ plays the same role as before. This can be solved by using the appropriate powers of $\hbar$ and c. γ has now the following dimensional structure

$$[\gamma]=[\hbar^m][c^n]=kg^m\frac{m^{2m+n}}{s^{m+n}} \tag{A.22}$$

We can immediately see that m=8 and consequently, n=-14. Therefore $\gamma=\frac{\hbar^8}{c^{14}}$. The cross section in SI units is then

$$\sigma=\frac{973}{10125\pi}\alpha^4\left\{\frac{\hbar\omega}{mc^2}\right\}^6\left\{\frac{\hbar}{mc}\right\}^2 \tag{A.23}$$

Rotation of the polarization plane

To derive the expression for the rotation of the polarization plane in SI units we start with determining the units of the EH constants. Substituting all the SI units into expression A.20 we get

$$[c_1] = [c_2] = \frac{A^4 s^{10}}{kg^3 m^5} = \frac{C^4 s^6}{kg^3 m^5} \tag{A.24}$$

We have expressed the results now in Coulombs instead of Ampères. The polarization angle in natural HL units is

$$\Delta\psi_{QED} = (4c_1 - c_2)B^2\omega L = -\frac{6\alpha^2}{45m_e^4}B^2\omega L \tag{A.25}$$

Such that

$$\begin{gathered}[\Delta\psi_{QED}] = Rad = [\gamma][c_1][B^2][\omega][L] \\ [\gamma] = \frac{kgm^4}{C^2 s^3}\end{gathered} \tag{A.26}$$

Where γ now has the form

$$\begin{gathered}\gamma = \hbar^m c^n e^k \\ [\gamma] = kg^m C^k \frac{m^{2m+n}}{s^{m+n}}\end{gathered} \tag{A.27}$$

here e denotes the elementary charge of $1.602 \times 10^{-19} C$. We can see immediately that $m = 1$ and $k = -2$ such that $n = -2$. Therefore $\gamma = \frac{\hbar c^2}{e^2}$. In SI units the rotation of the polarization plane equals

$$\Delta\psi_{QED} = -\frac{6\alpha^2\hbar^4\epsilon_0^2}{45m_e^4 c^3 e^2}B^2\omega L \tag{A.28}$$

Appendix B

Derivations of equations

Modified Maxwell equations

We start by proving the derivative identities 3.17.

$$\begin{gathered}\mathcal{F} \equiv F_{\mu\nu}F^{\mu\nu} \\ \frac{\partial \mathcal{F}}{F_{\mu\nu}} = \frac{\partial F_{\mu\nu}}{\partial F_{\lambda\sigma}}F^{\mu\nu} + F_{\mu\nu}\frac{\partial F^{\mu\nu}}{\partial F_{\lambda\sigma}} = \delta^\lambda_\mu\delta^\sigma_\nu F^{\mu\nu} + F_{\mu\nu}\eta^{\mu\alpha}\eta^{\nu\beta}\frac{\partial F_{\alpha\beta}}{\partial F_{\lambda\sigma}} \\ = F^{\lambda\sigma} + F_{\mu\nu}\eta^{\mu\alpha}\eta^{\nu\beta}\delta^\lambda_\alpha\delta^\sigma_\beta = F^{\lambda\sigma} + \eta^{\mu\lambda}\eta^{\nu\sigma}F_{\mu\nu} = 2F^{\lambda\sigma}\end{gathered} \tag{B.1}$$

The proof of the other identity is almost the same.

$$\begin{gathered}\mathcal{G} \equiv F_{\mu\nu}\tilde{F}^{\mu\nu} \\ \frac{\partial \mathcal{G}}{\partial F_{\lambda\sigma}} = \frac{\partial F_{\mu\nu}}{\partial F_{\lambda\sigma}}\tilde{F}^{\mu\nu} + F_{\mu\nu}\frac{\partial \tilde{F}^{\mu\nu}}{\partial F_{\lambda\sigma}} = \delta^\lambda_\mu\delta^\sigma_\nu\tilde{F}^{\mu\nu} + F_{\mu\nu}\frac{1}{2}\epsilon^{\mu\nu\alpha\beta}\frac{\partial F_{\alpha\beta}}{\partial F_{\lambda\sigma}} \\ = \tilde{F}^{\lambda\sigma} + \frac{1}{2}\epsilon^{\mu\nu\alpha\beta}\frac{\partial F_{\alpha\beta}}{\partial F_{\lambda\sigma}} = \tilde{F}^{\lambda\sigma} + \frac{1}{2}\epsilon^{\mu\nu\alpha\beta}\delta^\lambda_\alpha\delta^\sigma_\beta \\ = \tilde{F}^{\lambda\sigma} + \frac{1}{2}\epsilon^{\mu\nu\lambda\sigma}F_{\mu\nu} = \tilde{F}^{\lambda\sigma} + \tilde{F}^{\lambda\sigma} = 2\tilde{F}^{\lambda\sigma}\end{gathered} \tag{B.2}$$

Here we used the definition of the dual tensor. The EH Lagrangian is a function of the field tensor only. The field tensor only depends on derivatives of A^μ, which means the EH Lagrangian depends on derivatives of A^μ only. Therefore, the EL equations of motion for fields reduce to

$$\partial_\mu\frac{\partial \mathcal{L}}{\partial(\partial_\mu A_\nu)} - \frac{\partial \mathcal{L}}{\partial A_\nu} = \partial_\mu\frac{\partial \mathcal{L}}{\partial(\partial_\mu A_\nu)} = \partial_\mu\frac{\partial \mathcal{L}}{F_{\mu\nu}} = 0 \tag{B.3}$$

We write the EH Lagrangian in terms of $\mathcal{F}$ and $\mathcal{G}$ in natural HL units.

$$\mathcal{L}_{EH} = -\frac{1}{4}\mathcal{F} + \frac{2\alpha^2}{45m_e^4}\mathcal{F}^2 + \frac{14\alpha^2}{45m_e^4}\mathcal{G}^2 \tag{B.4}$$

Using the identities proven above, the modified equations of motion are

$$\begin{gathered}\partial_\mu\frac{\partial \mathcal{L}_{EH}}{F_{\mu\nu}} = \partial_\mu(-\frac{1}{2}F^{\mu\nu} + \frac{2\alpha^2}{45m_e^4}4\mathcal{F}F^{\mu\nu} + \frac{14\alpha^2}{45m_e^4}4\mathcal{G}\tilde{F}^{\mu\nu}) \\ = -\frac{1}{2}\partial_\mu F^{\mu\nu} + \frac{2\alpha^2}{45m_e^4}\partial_\mu(4(F_{\alpha\beta}F^{\alpha\beta})F^{\mu\nu} + 28(F_{\alpha\beta}\tilde{F}^{\alpha\beta})\tilde{F}^{\mu\nu}) = 0 \\ \partial_\mu F^{\mu\nu} = \frac{4\alpha^2}{45m_e^4}\partial_\mu(4(F_{\alpha\beta}F^{\alpha\beta})F^{\mu\nu} + 28(F_{\alpha\beta}\tilde{F}^{\alpha\beta})\tilde{F}^{\mu\nu})\end{gathered} \tag{B.5}$$

Equations of motions including axions

In the case of axions the Lagrangian becomes

$$\mathcal{L} = \mathcal{L}_{EH} + \frac{1}{2}\Big\{(\partial_\mu\phi)^2 - m^2\phi^2\Big\} - \frac{G}{4}\phi\Big\{\delta_{a,s}(E^2 - B^2) + \delta_{a,p}(\vec{E}\cdot\vec{B})\Big\} \quad , a = s, p$$
$$(\partial_\mu\phi)^2 \equiv \partial_\mu\phi\partial^\mu\phi \tag{B.6}$$

In this case we have two fields (ϕ and A^μ), yielding two equations of motion. Starting with ϕ we get from the EL equations of motion

$$\begin{aligned}
\partial_\tau\frac{\partial\mathcal{L}}{\partial(\partial_\tau\phi)} - \frac{\partial\mathcal{L}}{\partial\phi} &= \partial_\tau\Big\{\frac{1}{2}\frac{\partial(\partial_\mu\phi)}{\partial(\partial_\tau\phi)}\partial^\mu\phi + \frac{1}{2}\partial_\mu\phi\frac{\partial(\partial(\partial^\mu\phi)}{\partial(\partial_\tau\phi)}\Big\} + m^2\phi + \frac{G}{4}\Big\{\delta_{a,s}F^{\mu\nu}F_{\mu\nu} + \delta_{a,p}\tilde{F}^{\mu\nu}F_{\mu\nu}\Big\} \\
&= \partial_\tau\Big\{\frac{1}{2}\delta^\tau_\mu\partial^\mu\phi + \frac{1}{2}\partial_\mu\phi\eta^{\mu\lambda}\delta^\tau_\lambda\Big\} + m^2\phi + \frac{G}{4}\Big\{\delta_{a,s}F^{\mu\nu}F_{\mu\nu} + \delta_{a,p}\tilde{F}^{\mu\nu}F_{\mu\nu}\Big\} \\
&= \partial_\tau\Big\{\frac{1}{2}\partial^\tau + \frac{1}{2}\eta^{\mu\tau}\partial_\mu\phi\Big\} + m^2\phi + \frac{G}{4}\Big\{\delta_{a,s}F^{\mu\nu}F_{\mu\nu} + \delta_{a,p}\tilde{F}^{\mu\nu}F_{\mu\nu}\Big\} \\
&= \partial_\tau\partial^\tau\phi + m^2\phi + \frac{G}{4}\Big\{\delta_{a,s}F^{\mu\nu}F_{\mu\nu} + \delta_{a,p}\tilde{F}^{\mu\nu}F_{\mu\nu}\Big\} = 0 \\
\Box\phi + m^2\phi &= -\frac{G}{4}\Big\{\delta_{a,s}F^{\mu\nu}F_{\mu\nu} + \delta_{a,p}\tilde{F}^{\mu\nu}F_{\mu\nu}\Big\}
\end{aligned} \tag{B.7}$$

which is an inhomogeneous Klein-Gordon equation. The equation of motion for A^μ is the equation of motion derived above plus an axion contribution.

$$\begin{aligned}
\partial_\mu\frac{\partial\mathcal{L}}{\partial F_{\mu\nu}} &= \partial_\mu\frac{\partial\mathcal{L}_{EH}}{\partial F_{\mu\nu}} + \frac{G}{2}\partial_\mu\phi\Big\{\delta_{a,s}F^{\mu\nu} + \delta_{a,p}\tilde{F}^{\mu\nu}\Big\} = 0 \\
\partial_\mu F^{\mu\nu} - \frac{4\alpha^2}{45m_e^4}\partial_\mu(4(F_{\alpha\beta}F^{\alpha\beta})F^{\mu\nu} + 28(F_{\alpha\beta}\tilde{F}^{\alpha\beta})\tilde{F}^{\mu\nu}) + G\partial_\mu\phi\Big\{\delta_{a,s}F^{\mu\nu} + \delta_{a,p}\tilde{F}^{\mu\nu}\Big\} &= 0 \\
\partial_\mu F^{\mu\nu} = \frac{4\alpha^2}{45m_e^4}\partial_\mu(4(F_{\alpha\beta}F^{\alpha\beta})F^{\mu\nu} + 28(F_{\alpha\beta}\tilde{F}^{\alpha\beta})\tilde{F}^{\mu\nu}) - G\partial_\mu\phi\Big\{\delta_{a,s}F^{\mu\nu} + \delta_{a,p}\tilde{F}^{\mu\nu}\Big\}
\end{aligned} \tag{B.8}$$

Classical and modified wave equations

The classical wave equations follow almost directly from the classical Maxwell equations. Applying the curl to Faraday's gives

$$\begin{aligned}
\nabla\times(\nabla\times\vec{E}) &= -\nabla\times\frac{\partial B}{\partial t} \\
\nabla(\nabla\cdot\vec{E}) - \nabla^2 E &= -\frac{\partial}{\partial t}\nabla\times\vec{B} \\
\nabla^2 E &= \epsilon_0\mu_0\frac{\partial^2 E}{\partial t^2}
\end{aligned} \tag{B.9}$$

In the second line the first term vanishes due to Gauss's law. The derivation for the wave equation of the magnetic field is almost the same. Applying the curl to

Ampère's gives

$$\begin{aligned}\nabla \times (\nabla \times \vec{B}) &= \nabla \times (\epsilon_0 \mu_0 \frac{\partial E}{\partial t}) \\ \nabla(\nabla \cdot \vec{B}) - \nabla^2 B &= \epsilon_0 \mu_0 \frac{\partial}{\partial t} \nabla \times \vec{E} \\ \nabla^2 &= \epsilon_0 \mu_0 \frac{\partial B}{\partial t^2}\end{aligned} \tag{B.10}$$

The derivation of the wave equations including non-linear QED corrections uses the same tricks. Let's start with the wave equation for the electric field. Gauss's law now takes the form

$$\begin{aligned}\nabla \cdot \vec{D} &= \nabla \cdot \vec{E} + \nabla \cdot \vec{P}_{vac} = 0 \\ \nabla \cdot \vec{E} &= -\nabla \cdot \vec{P}_{vac}\end{aligned} \tag{B.11}$$

The expression for the polarization of the vacuum is found through the constitutive relation for the electric displacement. We have calculated this in chapter 3. Applying again the curl to Faraday's law gives

$$\begin{aligned}\nabla \times (\nabla \times \vec{E}) &= -\nabla \times \frac{\partial B}{\partial t} \\ \nabla(\nabla \cdot \vec{E}) - \nabla^2 E &= -\frac{\partial}{\partial t} \nabla \times \vec{B} \\ \nabla(-\nabla \cdot \vec{P}_{vac}) - \nabla^2 E &= -\frac{\partial}{\partial t}(\nabla \times (\vec{H} + \vec{M}_{vac})) \\ \nabla(-\nabla \cdot \vec{P}_{vac}) - \nabla^2 E &= -\frac{\partial}{\partial t}(\frac{\partial D}{\partial t} + \nabla \times \vec{M}_{vac}) \\ \nabla(-\nabla \cdot \vec{P}_{vac}) - \nabla^2 E &= -\frac{\partial}{\partial t}(\frac{\partial E}{\partial t} + \frac{\partial P_{vac}}{\partial t} + \nabla \times \vec{M}_{vac})\end{aligned} \tag{B.12}$$

Rearranging the terms to get the structure of a wave equation for the electric field we get

$$\frac{\partial^2 E}{\partial t^2} - \nabla^2 E = \Box E = \nabla(\nabla \cdot \vec{P}_{vac}) - \frac{\partial^2 P_{vac}}{\partial t^2} - \frac{\partial}{\partial t}(\nabla \times \vec{M}_{vac}) \tag{B.13}$$

Starting point for the modified wave equation for the magnetic field is again Ampère's law.

$$\begin{aligned}\nabla \times \vec{H} = \nabla \times \vec{B} - \nabla \times \vec{M}_{vac} &= \frac{\partial E}{\partial t} + \frac{\partial P_{vac}}{\partial t} \\ \nabla \times \vec{B} &= \frac{\partial E}{\partial t} + \frac{\partial P_{vac}}{\partial t} + \nabla \times \vec{M}_{vac} \\ \nabla \times (\nabla \times \vec{B}) &= \frac{\partial}{\partial t}(\nabla \times \vec{E}) + \frac{\partial}{\partial t}(\nabla \times \vec{P}_{vac}) + \nabla \times (\nabla \times \vec{M}_{vac}) \\ \nabla(\nabla \cdot \vec{B}) - \nabla^2 B &= -\frac{\partial^2 B}{\partial t^2} + \frac{\partial}{\partial t}(\nabla \times \vec{P}_{vac}) + \nabla \times (\nabla \times \vec{M}_{vac}) \\ \Box B &= \frac{\partial}{\partial t}(\nabla \times \vec{P}_{vac}) + \nabla \times (\nabla \times \vec{M}_{vac})\end{aligned} \tag{B.14}$$

which is the modified wave equation for the magnetic field.

Bibliography

[1] *David Tong, lecture notes on quantum field theory.* 2006-2007.

[2] *David J. Griffiths, Introduction to electrodynamics.* Pearson, 2014.

[3] *Eugene Hecht, Optics.* Pearson, 2014.

[4] Adil Aktas, E Rizvi, A Lebedev, A Rostovtsev, C Pascaud, D Lüke, JG Contreras, M Gregori, C Kiesling, W Yan, et al. Elastic j/psi production at hera. *Eur. Phys. J. C*, 46(hep-ex/0510016):585–603, 2005.

[5] Gerald W Bennett, B Bousquet, HN Brown, G Bunce, RM Carey, P Cushman, GT Danby, PT Debevec, M Deile, H Deng, et al. Final report of the e821 muon anomalous magnetic moment measurement at bnl. *Physical Review D*, 73(7):072003, 2006.

[6] Vladimir Borisovich Berestetskii, Evgenii Mikhailovich Lifshitz, and Pitaevskiĭ. *Quantum electrodynamics.*

[7] Zvi Bern, Abilio De Freitas, Adrian Ghinculov, Henry Wong, and Lance Dixon. Qcd and qed corrections to light-by-light scattering. *Journal of High Energy Physics*, 2001(11):031, 2001.

[8] Iwo Bialynicki-Birula. Nonlinear structure of the electromagnetic vacuum. *Physica Scripta*, 21:22–26, 1988.

[9] Max Born and Emil Wolf. *Principles of optics: electromagnetic theory of propagation, interference and diffraction of light.* Elsevier, 2013.

[10] Davide Cadamuro. Cosmological limits on axions and axion-like particles. *arXiv preprint arXiv:1210.3196*, 2012.

[11] ATLAS collaboration. Evidence for light-by-light scattering in heavy-ion collisions with the atlas detector at the lhc.

[12] Michael Dine, Willy Fischler, and Mark Srednicki. A simple solution to the strong cp problem with a harmless axion. *Physics letters B*, 104(3):199–202, 1981.

[13] Gerald V Dunne. Heisenberg-euler effective lagrangians: basics and extensions. *From Fields to Strings: Circumnavigating Theoretical Physics*, 1:445, 2005.

[14] Gerald V Dunne. New strong-field qed effects at eli: nonperturbative vacuum pair production. *arXiv preprint arXiv:0812.3163*, 2008.

[15] Gerald V Dunne. The heisenberg–euler effective action: 75 years on. *International Journal of Modern Physics A*, 27(15):1260004, 2012.

[16] Thomas Erber. High-energy electromagnetic conversion processes in intense magnetic fields. *Reviews of Modern Physics*, 38(4):626, 1966.

[17] Jonathan L Feng, Bartosz Fornal, Iftah Galon, Susan Gardner, Jordan Smolinsky, Tim MP Tait, and Philip Tanedo. Protophobic fifth-force interpretation of the observed anomaly in be 8 nuclear transitions. *Physical review letters*, 117(7):071803, 2016.

[18] Enrico Fermi. On the theory of collisions between atoms and electrically charged particles. *arXiv preprint hep-th/0205086*, 2002.

[19] Ramandeep Gill and Jeremy S Heyl. Constraining the photon-axion coupling constant with magnetic white dwarfs. *Physical Review D*, 84(8):085001, 2011.

[20] W Heisenberg and H Euler. Consequences of dirac theory of the positron. *arXiv preprint physics/0605038*, 2006.

[21] Jeremy S Heyl and Nir J Shaviv. Polarization evolution in strong magnetic fields. *Monthly Notices of the Royal Astronomical Society*, 311(3):555–564, 2000.

[22] G Jarlskog, L Jönsson, S Prünster, HD Schulz, HJ Willutzki, and GG Winter. Measurement of delbrück scattering and observation of photon splitting at high energies. *Physical Review D*, 8(11):3813, 1973.

[23] Robert Karplus and Maurice Neuman. The scattering of light by light. *Physical Review*, 83(4):776, 1951.

[24] B King and T Heinzl. Measuring vacuum polarization with high-power lasers. *High Power Laser Science and Engineering*, 4:e5, 2016.

[25] SI Kruglov. Vacuum birefringence from the effective lagrangian of the electromagnetic field. *Physical Review D*, 75(11):117301, 2007.

[26] A.D. Polosa L.M. Capparelli, L. Maiani. A note on polarized light from magnetars: Qed effects and axion-like particles.

[27] Mattias Marklund and Joakim Lundin. Quantum vacuum experiments using high intensity lasers. *The European Physical Journal D-Atomic, Molecular, Optical and Plasma Physics*, 55(2):319–326, 2009.

[28] Peter Mészáros. *High-energy radiation from magnetized neutron stars*. University of Chicago press, 1992.

[29] RP Mignani, V Testa, D González Caniulef, R Taverna, R Turolla, S Zane, and K Wu. Evidence for vacuum birefringence from the first optical-polarimetry measurement of the isolated neutron star rx j1856. 5- 3754. *Monthly Notices of the Royal Astronomical Society*, 465(1):492–500, 2017.

[30] Javier Redondo and Andreas Ringwald. Light shining through walls. *Contemporary Physics*, 52(3):211–236, 2011.

[31] Soroush Shakeri, Mansour Haghighat, and She-Sheng Xue. Nonlinear qed effects in x-ray emission of pulsars. *arXiv preprint arXiv:1704.04750*, 2017.

[32] Selym Villalba-Chávez and Antonino Di Piazza. Axion-induced birefringence effects in laser driven nonlinear vacuum interaction. *arXiv preprint arXiv:1307.7935*, 2013.

[33] DA Williams, D Antreasyan, HW Bartels, D Besset, Ch Bieler, JK Bienlein, A Bizzeti, ED Bloom, I Brock, K Brockmüller, et al. Formation of the pseudoscalars π 0, η, and η'in the reaction $\gamma\gamma \rightarrow \gamma\gamma$. *Physical Review D*, 38(5):1365, 1988.

[34] E Zavattini, G Zavattini, G Ruoso, G Raiteri, E Polacco, E Milotti, V Lozza, M Karuza, U Gastaldi, G Di Domenico, et al. New pvlas results and limits on magnetically induced optical rotation and ellipticity in vacuum. *Physical Review D*, 77(3):032006, 2008.